TABLE 2
The Frequency of Alcohol Dehydrogenase 3, Aldehyde Dehydrogenase 2, and Cytochrome P450 2E1 Genotypes and Odds Ratios Among Lung Cancer Cases and Controls

Genotype	No. (%)		OR	
	Cases (n = 505)	Controls (n = 256)	Crude	Adjusted*
ADH₃				
C/C	459 (90.9)	227 (88.7)	1	1
C/V	44 (8.7)	29 (11.3)	0.75 (0.46–1.23)	0.71 (0.40–1.16)
V/V	2 (0.4)	0 (0)	—	—
C/V and V/V	46 (9.1)	29 (11.3)	0.78 (0.48–1.28)	0.74 (0.44–1.24)
ALDH₂				
C/C	319 (63.2)	134 (52.3)	1	1
C/V	168 (33.3)	108 (42.2)	0.65 (0.48–0.90)†	0.73 (0.52–1.03)
V/V	18 (3.6)	14 (5.5)	0.54 (0.26–1.12)	0.75 (0.35–1.59)
C/V and V/V	186 (36.8)	122 (47.7)	0.64 (0.47–0.87)†	0.73 (0.53–1.02)
CYP2E1				
C/C	300 (59.4)	147 (57.4)	1	1
C/V	175 (34.7)	106 (41.4)	0.81 (0.59–1.11)	0.83 (0.60–1.15)
V/V	30 (5.9)	3 (1.2)	4.90 (1.47–16.32)†	4.66 (1.36–16.0)†
C/V and V/V	205 (40.6)	109 (42.6)	0.92 (0.68–1.25)	0.93 (0.68–1.29)

OR indicates odds ratios; *ADH₃*, alcohol dehydrogenase 3; C, common allele; V, variant allele; *ALDH₂*, aldehyde dehydrogenase 2; *CYP2E1*, cytochrome P450 2E1.
* ORs were adjusted for age, sex, smoking amounts (pack-years), and alcohol amounts (ethanol: mg per day).
† $P < .05$.

shown in Table 3. Drinking was classified as none, light (31.6 g per day) or heavy (>31.6 g per day). When adjusted for age, sex, and smoking amounts, drinking imposed a significantly greater risk of lung cancer occurrence. The ORs for the light drinkers and heavy drinkers, compared with nondrinkers, were 1.76 and 1.95, respectively (P for trend = .012). Thus, the risk of lung cancer increases as the amount alcohol consumed increases.

ORs for developing lung cancer in association with the *ADH₃*, *ALDH₂*, and *CYP2E1* genotypes also are presented in Table 3. Similar to what was observed in all participants taken together, an increased risk for developing lung cancer also was observed among individuals who were homozygous for the common allele ADH_3^{1-1}. However, because there were too few *ADH₃* variant allele carriers to analyze any association between alcohol consumption and lung cancer risk for this allele, it was inappropriate to compare the ADH_3^2 and ADH_3^{1-1} genotypes.

The adjusted OR for the $ALDH_2^{1-1}$ group was 0.75 (95% CI, 0.39–1.42) in light drinkers and 0.46 (95% CI, 0.20–0.99) in heavy drinkers. In contrast, individuals with the $ALDH_2^2$ allele had a significantly greater risk of lung cancer; light drinkers had a 3.6-fold increased risk, and heavy drinkers had a 6.2-fold increased risk compared with nondrinkers (P for trend < .0001). These results indicate that, in individuals with the *ALDH₂* variant allele, continuous alcohol consumption is a strong risk factor for lung cancer.

The OR for the *CYP2E1* c1/c1 genotype was 1.81 (95% CI, 0.97–3.38) for light drinkers and 1.67 (95% CI, 0.86–3.21) for heavy drinkers. For individuals with the *CYP2E1* c2 allele, the OR was 1.74 (95% CI, 0.91–3.35) for light drinkers and 2.56 (95% CI, 1.16–5.65) for heavy drinkers (P for trend = .005). These results may indicate that individuals with the *CYP2E1* variant allele are in a high-risk group for lung cancer in heavy drinkers.

It must be emphasized that, because of differences in distribution according to sex between cases and controls, we analyzed relative risks only in men (Table 4). For baseline characteristics among men, higher consumption of alcohol and more smoking were observed, as expected. Regarding associations between alcohol consumption and lung cancer risk, drinking was associated with an increased risk of developing lung cancer in all participants. The adjusted OR for the light and drinkers, compared with nondrinkers, was 6.54 (95% CI, 3.13–13.7) and 6.58 (95% CI, 3.28–13.2), respectively. However, in individuals with active $ALDH_2^{1-1}$ genotypes, there was no association between alcohol consumption and lung cancer risk. In individuals with the inactive $ALDH_2^2$ alleles, the risk for lung cancer was 6.8-fold (95% CI, 2.72–17.1) for light drinkers and 9.3-fold (95% CI, 3.72–23.4) for heavy drinkers compared with nondrinkers (P for trend <.0001). The risk in men who were heavy drinkers was much greater compared with women and those who carried the active $ALDH_2^{1-1}$ genotype.

In individuals with the c2 allele, the risk of lung cancer for light drinkers (OR, 8.31; 95% CI, 2.67–25.9) and for heavy drinkers (OR, 9.93; 95% CI, 3.39–29.1) was increased compared with individuals who were homozygous for the *CYP2E1* c1 allele and compared with the risks in all men. However, it should be noted that, because of the low incidence of homozygosity for variant allele in the control group, statistical power was limited in this instance. Similar assessments also were made in women, but no significant associations between any genotype and lung cancer risk were observed (data not shown).

Table 5 shows the distribution of the *ADH₃*, *ALDH₂*, and *CYP2E1* genotypes according to tumor histology. The frequency of the ADH_3^2 allele for all histologic types was similar to the frequency observed in controls. The frequency of the $ALDH_2^2$ allele for squamous cell carcinomas, small cell carci-

TABLE 3
Odds Ratios of Developing Lung Cancer for Alcohol Dehydrogenase 3, Aldehyde Dehydrogenase 2, and Cytochrome P450 2E1 Genotypes Stratified by Drinking Amounts

			Drinkers						
	Nondrinkers		31.6 g/Day			>31.6 g/Day			
Genotype	No.*	Reference	No.*	OR (95% CI)†	P	No.*	OR (95% CI)†	P	P for trend‡
All	120/119	1	154/65	1.76 (1.12–2.75)	.014	231/72	1.95 (1.19–3.21)	.0085	.012
ADH_3									
C/C	112/105	1	141/60	1.59 (0.99–2.55)	.054	206/62	1.88 (1.10–3.21)	.02	.025
C/V and V/V	8/14	1	13/5	4.31 (0.912–20.38)	.065	25/10	3.28 (0.742–14.55)	.12	.17
$ALDH_2$									
C/C	57/41	1	99/39	0.75 (0.39–1.42)	.37	163/54	0.46 (0.2–0.99)	.049	.03
C/V and V/V	63/78	1	55/26	3.63 (1.76–7.46)	.0005	68/18	6.15 (2.77–13.65)	<.0001	<.0001
CYP2E1									
C/C	72/61	1	95/36	1.81 (0.97–3.38)	.061	133/50	1.67 (0.86–3.21)	.13	.31
C/V and V/V	48/58	1	59/29	1.74 (0.91–3.35)	.097	98/22	2.56 (1.16–5.65)	.02	.005

OR indicates odds ratio; 95% CI, 95% confidence interval; *ADH_3*, alcohol dehydrogenase 3; C, common allele; V, variant allele; *$ALDH_2$*, aldehyde dehydrogenase 2; *CYP2E1*, cytochrome P450 2E1.
* The number of cases/number of controls.
† ORs were adjusted for age, sex, and smoking amount (pack-years).
‡ The Mantel extension test.

TABLE 4
Odds Ratios of Developing Lung Cancer for Alcohol Dehydrogenase 3, Aldehyde Dehydrogenase 2, and Cytochrome P450 2E1 Genotypes Stratified by Drinking Amounts Among Men

			Drinkers						
	Nondrinkers		31.6 g/Day			>31.6 g/Day			
Genotype	No.*	Reference	No.*	OR (95% CI)†	P	No.*	OR (95% CI)†	P	P for Trend‡
All	17/31	1	120/36	6.54 (3.13–13.65)	<.0001	223/59	6.58 (3.28–13.22)	.0001	<.0001
ADH_3									
C/C	15/27	1	110/34	6.14 (2.83–13.29)	<.0001	201/49	7.27 (3.44–15.36)	.0001	<.0001
C/V and V/V	2/4	1	10/2	23.31(1.41–286.0)	.028	22/10	5.43 (0.63–47.09)	.12	.47
$ALDH_2$									
C/C	5/2	1	72/16	1.47 (0.25–8.67)	.67	158/42	1.10 (0.20–6.23)	.91	.29
C/V and V/V	12/29	1	48/20	6.82 (2.72–17.13)	<.0001	65/17	9.33 (3.72–23.39)	.0001	<.0001
CYP2E1									
C/C	10/14	1	77/24	5.22 (1.95–13.94)	.0003	125/42	4.71 (1.85–12.05)	.0012	.08
C/V and V/V	7/17	1	43/12	8.31 (2.67–25.89)	.0001	98/17	9.93 (3.39–29.09)	.0001	<.0001

OR indicates odds ratio; 95% CI, 95% confidence interval; *ADH_3*, alcohol dehydrogenase 3; C, common allele; V, variant allele; *$ALDH_2$*, aldehyde dehydrogenase 2; *CYP2E1*, cytochrome P450 2E1.
* Values shown represent the number of cases/number of controls.
† OR were adjusted for age, sex, and smoking history (pack-years).
‡ Mantel extension test.

nomas, and other histologic types was similar to that observed in controls. However, the *$ALDH_2^2$* allele was significantly less common in patients with adenocarcinomas than in controls (36.1% vs 47.7%; $P = .018$). In contrast, the *CYP2E1* c2/c2 genotype was more common in patients with adenocarcinomas (5.8%) and small cell carcinomas (9.8%) than in controls (1.2%).

In this study, we observed that alcohol consumption was an independent risk factor for lung cancer after adjusting for the influence of smoking (P for trend = .012). Although we assumed that individuals who had the *ADH_3^{1-1}* genotype were at greater risk for lung cancer compared with individuals who had the *ADH_3^2* allele, there was no evidence of an association between lung cancer and the *ADH_3* genotype

TABLE 5
Distribution of Alcohol Dehydrogenase 3, Aldehyde Dehydrogenase 2, and Cytochrome P450 2E1 Genotype According to Histologic Findings

	No. (%)				
		Histologic type			
Genotype	Control group (n = 256)	Adenocarcinoma (n = 330)	Squamous cell (n = 100)	Small cell (n = 51)	Other (n = 24)
ADH_3					
C/C	227 (88.3)	297 (90)	91 (91)	48 (94.1)	23 (95.8)
C/V	29 (11.7)	31 (9.4)	9 (9)	3 (5.9)	1 (4.2)
V/V	0 (0)	2 (0.6)	0 (0)	0 (0)	0 (0)
P for difference*		.35	.52	.25	.28
$ALDH_2$					
C/C	134 (52.3)	211 (63.9)	54 (54)	36 (70.6)	18 (75)
C/V	108 (42.2)	104 (31.5)	45 (45)	13 (25.5)	6 (25)
V/V	14 (5.5)	15 (4.6)	1 (1)	2 (3.9)	0 (0)
P for difference*		.018	.17	.056	.083
CYP2E1					
C/C	147 (57.4)	197 (59.7)	59 (59)	31 (60.8)	13 (54.2)
C/V	106 (41.4)	114 (34.6)	37 (37)	15 (29.4)	9 (37.5)
V/V	3 (1.2)	19 (5.8)	4 (4)	5 (9.8)	2 (8.3)
P for difference*		.0067	.19	.001	.04

ADH_3 indicates alcohol dehydrogenase 3; C, common allele; V, variant allele; $ALDH_2$, aldehyde dehydrogenase 2; *CYP2E1*C, cytochrome P450 2E1.
* Chi-square test for comparison with controls.

in any analysis. Because the enzyme activity of $ALDH_2^2$ is extremely low, acetaldehyde accumulates after alcohol intake. We could not demonstrate any association of $ALDH_2$ genotypes with the risk of lung cancer after adjusting for smoking and the amount of alcohol consumed. However, we observed that individuals who had the $ALDH_2^2$ allele were at a significantly greater risk of lung cancer because of alcohol consumption, although there was a significant trend for lower levels of alcohol consumption in individuals who had the $ALDH_2^{1-1}$ genotype (P for trend = .03). We hypothesized that not only the differences in blood acetaldehyde concentrations but also the differences in enzyme activity on tobacco-specific carcinogens contribute to carcinogenesis. However, we produced no evidence that lung cancer risk is related to possession of the *CYP2E1* c2/c2 genotype or that the *CYP2E1* genotype modifies lung cancer susceptibility related to alcohol intake.

DISCUSSION

The control population for this study was recruited from the visitors to the NCCH-E. The majority of patients had false-positive chest x-rays at their annual check-up and had normal chest computed tomography scans, and they were not suffering from any respiratory illness. Furthermore, their family medical histories were similar to those expected in the ordinary Japanese population, although the number of current smokers among both men (42.9%) and women (6.9%) may have been somewhat lower than the average (46.8% and 11.1%, respectively, for 2003 according to the Announcement of the Ministry of Health, Labor, and Welfare). For these reasons, we believe that our control group was not at greater risk of cancer occurrence compared with the regular Japanese population. Moreover, it was not necessary to take into account any biases stemming from the selective inclusion only of consenting participants, because the great majority of both patients and controls agreed to participate in the study.

The data from the control group showed that individuals who had the $ALDH_2$ wild-type genotype consumed more alcohol than individuals who had the variant genotype. This may suggest that genetic polymorphisms of alcohol-metabolizing enzymes influence drinking habits, because consumption may be limited by the unpleasant reactions caused by the accumulation of acetaldehyde in individuals with $ALDH_2$ variant genotypes. Nonetheless, habitual drinking can increase consumption because of increased microsomal acetaldehyde-oxidizing system activation, further promoting the oxidation of acetaldehyde. The association between drinking habit and ADH_3 and *CYP2E1* genotypes remains uncertain.

Regarding correlations between smoking and drinking habits, the coexistence of smoking and

drinking increased the risk of lung cancer compared with nondrinkers who never smoked, particularly the OR for heavy smokers (>37 pack-years) and drinkers, which was 8.4 (95% CI, 2.3–30.2; $P = .0012$) in the light drinkers and 7.0 (95% CI, 2.1–23.4) in the heavy drinkers (data not shown).

The involvement of alcohol in lung cancer etiology has been controversial, although many epidemiologic studies have suggested positive associations between different parameters of alcohol consumption and lung cancer risk. In the current study, we have demonstrated that drinking is a strong risk factor for lung cancer that is dose-dependent and is stronger in men than in women. This same tendency was observed even in the genotype analysis, but none of the results indicated a significant association between lung cancer and drinking in women. Furthermore, no associations were observed between peripheral lung adenocarcinoma, drinking, and genotypes of alcohol metabolite-related enzymes in women.

The question of ethnicity in the distribution of the polymorphisms of these alcohol metabolite-related enzyme genes always must be considered. The ADH_3^2 allele is present in almost 60% of whites but is far more rare (5–10%) in Japanese. In contrast, the $ALDH_2^2$ allele is found only in Asians. The *CYP2E1* c2 allele is present in 35% to 56% of Japanese and Chinese, and in 2% to 5% of whites. In the current study, the frequency of variant alleles of each polymorphism was 9.9% for ADH_3, 40.5% for $ALDH_2$, and 41.3% for *CYP2E1*. This is consistent with previous studies in Japanese and other Asians.

We observed that the risk for lung cancer was increased significantly by alcohol consumption in a dose-dependent fashion in individuals with the $ALDH_2^2$ alleles. Previously, some Japanese studies also showed a strong genetic and environmental interaction between $ALDH_2^2$ and alcohol intake for the risk of developing esophageal and upper aerodigestive tract cancer.[18–21] In contrast, for individuals with the $ALDH_2^{1-1}$ genotype, there was an inverse association between alcohol consumption and the risk of lung cancer. These results suggest that increased acetaldehyde concentrations from a reduction in acetaldehyde oxidation caused by the presence of the $ALDH_2^2$ allele contribute to the development of lung cancer. Significantly higher blood acetaldehyde concentrations after drinking in individuals with the ADH_3^1 or $ALDH_2^2$ allele have been reported compared with the concentrations in individuals who lacked these alleles,[11,29] and it has been demonstrated that breath acetaldehyde levels are proportional to blood acetaldehyde levels. Indeed, Muto et al.[30] and Jones[31] observed significantly higher acetaldehyde levels in the breath from individuals with the $ALDH_2^2$ allele than in those without that allele. Therefore, exposure to higher concentrations of acetaldehyde in the lower respiratory tract may play a critical role in alcohol-related carcinogenesis. Regarding the influence of smoking, when adjusted for age, sex, and amount of alcohol consumed, the risks for developing lung cancer in current smokers were 1.5-fold greater for those with the inactive $ALDH_2$ genotype (data not shown) compared with nonsmokers. The lung cancer risk for individuals with the $ALDH_2^2$ allele was not increased further by smoking.

Although there have been some reports of a significant association between the ADH_3^1 allele and some types of upper aerodigestive tract cancer, this association has been controversial.[16,17,32–34] We failed to observe an association between ADH_3 gene polymorphisms and the development of lung cancer, most likely because of the limited statistical power from the low frequency of the variant allele in the Japanese population.

Several investigations[24,31,35,36] have indicated that the *CYP2E1* c2 allele is associated with susceptibility to some types of cancer. However, other investigators reported that carriers of the c2 allele had decreased susceptibility to a number of cancers[25–27,37] and reported no association between *CYP2E1* genotypes and cancer.[23,28,38] Discrepancies among these results may be caused by several factors, including differences in study design, sample size, and the populations' ethnicity. Statistical power usually is very limited in studies of the white population because of the extreme rarity of variant genotypes. Although *CYP2E1* enzyme activity is induced by certain chemicals, such as ethanol, large interindividual variation has been observed in its constitutive activity as well as after induction. Watanabe et al.[39] and Hayashi et al.[15] reported that the *RsaI* variant c2 allele produced higher enzyme activity than the c1/c1 genotype in Japanese individuals, although this finding is itself controversial.[40–42] Highly activated *CYP2E1* induced by alcohol may play a more important role in the metabolic activation of several tobacco-specific procarcinogens, including various nitrosamines. It has been suggested that these low-molecular-weight carcinogens are associated with the development of peripheral adenocarcinoma. This finding is consistent with the results from our analysis of *CYP2E1* presented in Table 5. However, the *CYP2E1* c2/c2 genotype is not in Hardy-Weinberg equilibrium in the control population, the observed frequencies most likely are underestimates, and these findings of

an association with histologic type most likely are false-positive results. In our analysis of $ALDH_2$, the incidence of adenocarcinoma was high among individuals who had the wild-type genotype. Although a high incidence of squamous cell carcinoma was not observed, this result may imply that carcinogenesis caused by acetaldehyde occurs more in cancers other than adenocarcinoma as well as in esophageal and upper aerodigestive tract cancers.

A previous hospital-based study that was conducted in Japan failed to identify any association between the *RsaI* polymorphism and lung cancer, even when the analysis was stratified according to different histologic type.[28] A more recent study indicated that there was a significant decrease in overall lung cancer risk associated with the possession of at least 1 copy of the *CYP2E1 RsaI* variant allele, whereas there was no association between the *CYP2E1 RsaI* polymorphism and the histologic type of lung cancer.[27] However, none of the previous studies had adjusted for risk according to alcohol consumption levels, which strongly influence the activity of this enzyme. In the current study, we demonstrated that there is a difference between individuals who have the *CYP2E1 RsaI* c2/c2 genotype compared with individuals who have the common c1/c1 genotype, with an adjusted OR of 4.66 (95% CI, 1.36–16.0) for the former group. Because of the low incidence of homozygosity in controls, the genotype distribution was not in Hardy-Weinberg equilibrium in our control population. The increased lung cancer risk among individuals with the *CYP2E1* c2/c2 genotype likely was a false-positive result.

A correlation between the amount of alcohol consumed, genetic polymorphisms in the alcohol metabolite-related enzymes, and the stage of lung cancer was not observed in the current study, and we could not confirm that these factors were related to the aggressiveness of lung cancer. Furthermore, no associations were identified between the location of the primary cancer, the amount of alcohol consumed, and the genotype of these enzymes or between the risk for lung cancer and the type of alcoholic beverage consumed.

In summary, we report a significant association between amounts of alcohol consumed and susceptibility to lung cancer and that the risk of lung cancer in individuals with $ALDH_2$ variant alleles, but not with ADH_3 or *CYP2E1* variant alleles, apparently was enhanced more by alcohol intake than in individuals with common genotypes. Moreover, to our knowledge, this is the first report documenting an association between lung cancer and genetic polymorphisms of alcohol metabolite-related enzymes. Because the sample size was relatively small for the investigation of effects stratified by each genotype, the current findings should be confirmed in large-scale studies with greater statistical power.

REFERENCES

1. Bandera EV, Freudenheim JL, Vena JE. Alcohol consumption and lung cancer: a review of the epidemiologic evidence. *Cancer Epidemiol Biomarkers Prev.* 2001;10:813–821.
2. Glade MJ. Food, Nutrition and the Prevention of Cancer: A Global Perspective. American Institute for Cancer Research. *Nutrition.* 1999;6:523–526.
3. Bagnardi V, Blangiardo M, La Vecchia C, Corrao G. A meta-analysis of alcohol drinking and cancer risk. *Br J Cancer.* 2001;85:1700–1705.
4. International Agency for Research on Cancer. Allyl compounds, aldehyde, epoxies and peroxidies. *IARC Monogr Eval Carcinog Risks Hum.* 1985;36:101–132.
5. Delanco VL. A mutagenicity assessment of acetaldehyde. *Mutat Res.* 1998;195:1–20.
6. Helander A, Lindahl-Keissling K. Increased frequency of acetaldehyde-induced sister chromatic exchanges in human lymphocytes treated with an aldehyde dehydrogenase inhibitor. *Mutat Res.* 1991;264:103–107.
7. Woutersen RA, Applman LM, Van Garderen-Hoetmer A, Feron VJ. Inhalation toxicity of acetaldehyde in rat. III. Carcinogenicity study. *Toxicology.* 1986;41:213–231.
8. Feron VJ, Kruysse A, Woutersen RA. Respiratory tract tumors in hamsters exposed to acetaldehyde vapour alone or simultaneously to benzo[a]pyrene or diethylnitrosamine. *Eur J Cancer Clin Oncol.* 1982;18:13–31.
9. Kunitoh S, Imaoka S, Hiroi T, Yabusaki Y, Monna T, Funae Y. Acetaldehyde as well as ethanol is metabolized by human CYP2E1. *Pharmacol Exp Ther.* 1997;280:527–532.
10. Liber CS, DeCarli LM. Hepatic microsomal ethanol oxidizing system. *J Biol Chem.* 1970;254:2505–2512.
11. Bosron WF, Li TK. Genetic polymorphisms of human liver alcohol and aldehyde dehydrogenases and their relationship to alcohol metabolism and alcoholism. *Hepatology.* 1986;6:502–510.
12. Harada S, Misawa S, Agarwal DP, Goedde HW. Liver alcohol dehydrogenase and aldehyde dehydrogenase in Japanese: isozyme variation and its possible role in alcohol intoxication. *Am J Hum Genet.* 1980;32:8–15.
13. Sun F, Tsuritani I, Yamada Y. Contribution of genetic polymorphisms in ethanol-metabolizing enzymes to problem drinking behavior in middle-aged Japanese men. *Behav Genet.* 2002;32:229–236.
14. Iwahashi K, Miyatake R, Suwaki H, et al. Blood ethanol levels and the CYP2E1 C2 allele. *Arukoru Kenkyuto Yakubutsu Ison.* 1994;29:190–194.
15. Hayashi S, Watanabe J, Kawajiri K. Genetic polymorphism in 5'-flanking region change transcriptional regulation of the human cytochrome P-450IIE1 gene. *J Biochem.* 1991; 110:559–565.
16. Coutelle C, Ward PJ, Fleury B, et al. Laryngeal and oropharyngeal cancer and alcohol dehydrogenase 3 and glutathione S-transferase M1 polymorphisms. *Hum Genet.* 1997;99: 319–325.
17. Harty LC, Caporaso NE, Hayes RB, et al. Alcohol dehydrogenase 3 genotype and risk of oral cavity and pharyngeal cancers. *J Natl Cancer Inst.* 1997;89:1698–1705.

18. Yokoyama A, Muramatsu T, Ohmori T, Higuchi S, Hayashida M, Ishii H. Esophageal cancer and aldehyde dehydrogenase-2 genotype in Japanese males. *Cancer Epidemiol Biomarkers Prev.* 1996;5:99–102.
19. Hori H, Kawano T, Endo M, Yuasa Y. Genetic polymorphisms of tobacco- and alcohol-related metabolizing enzymes and human esophageal squamous cell carcinoma susceptibility. *J Clin Gastroenterol.* 1997;25:568–575.
20. Yokoyama A, Muramatsu T, Ohmori T, et al. Alcohol-related cancers and aldehyde dehydrogenase-2 in Japanese alcoholics. *Carcinogenesis.* 1998;19:1383–1387.
21. Nomura T, Noda H, Shibahara T, Yokoyama A, Muramatsu T, Ohmori T. Aldehyde dehydrogenase 2 and glutathione S-transferase M1 polymorphism in relation to the risk for oral cancer in Japanese drinkers. *Oral Oncol.* 2000;36:42–46.
22. Freudenhein JL, Ram M, Nie J, et al. Lung cancer in humans is not associated with lifetime total alcohol consumption or with genetic variation in alcohol dehydrogenase 3 (ADH_3)[1,2]. *J Nutr.* 2003;133:3619–3624.
23. Kato S, Shields PG, Caporaso NE, et al. Cytochrome P450IIE1 genetic polymorphisms, racial variation, and lung cancer risk. *Cancer Res.* 1992;52:6712–6715.
24. El-Zein RA, Zwischenberger JB, Abdel-Rahman SZ, Sankar AB, Au WW. Polymorphism of metabolizing genes and lung cancer histology: prevalence of CYP2E1 in adenocarcinoma. *Cancer Lett.* 1997;112:71–78.
25. Wu X, Shi H, Jiang H, et al. Association between cytochrome P4502E1 genotype, mutagen sensitivity, cigarette smoking and susceptibility to lung cancer. *Carcinogenesis.* 1997;18:967–973.
26. Persson I, Johansson I, Bergling H, et al. Genetic polymorphism of cytochrome P450 2E1 in a Swedish population: relationship to the incidence of lung cancer. *FEBS Lett.* 1993;319:207–211.
27. Marchand LL, Sivaraman L, Pierce L, et al. Association of CYP1A1, GSTM1, and CYP2E1 polymorphisms with lung cancer suggests cell type specificities to tobacco carcinogens. *Cancer Res.* 1998;68:4858–4863.
28. Watanabe J, Yang JP, Eguchi H, et al. An RsaI polymorphism in the CYP2E1 gene does not affect lung cancer risk in a Japanese population. *Jpn J Cancer Res.* 1995;86:245–248.
29. Yamamoto K, Ueno Y, Mizoi Y, Tatsuno Y. Genetic polymorphism of alcohol and aldehyde dehydrogenase and the effects on alcohol metabolism. *Arukoru Kenkyuto Yakubutu Ison.* 1993;28:3–25.
30. Muto M, Nakane M, Hitomi Y, et al. Association between aldehyde dehydrogenase gene polymorphisms and the phenomenon of field cancerization in patients with head and neck cancer. *Carcinogenesis.* 2002;23:1759–1765.
31. Jones AW. Measuring and reporting the concentration of acetaldehyde in human breath. *Alcohol Alcohol.* 1995;30:271–285.
32. Bouchardy C, Hirvonen A, Coutelle C, Ward PJ, Dayer P, Benhamou S. Role of alcohol dehydrogenase 3 and cytochrome P4502E1genotypes in susceptibility to cancers of upper aerodigestive tract. *Int J Cancer.* 2000;87:734–740.
33. Olshan AF, Weissler MC, Watson MA, Bell DA. Risk of head and neck cancer and the alcohol dehydrogenase-3 genotype. *Carcinogenesis.* 2001;22:57–61.
34. Sturgis EM, Dahlstrom KR, Guan Y, et al. Alcohol dehydrogenase 3 genotype is not associated with risk of squamous cell carcinoma of the oral cavity and pharynx. *Cancer Epidemiol Biomarkers Prev.* 2001;10:273–275.
35. Hung HC, Chuang J, Chien YC, et al. Genetic polymorphisms of CYP2E1, GSTM1, and GSTT1; environmental factors and risk of oral cancer. *Cancer Epidemiol Biomarkers Prev.* 1997;6:901–905.
36. Hildesheim A, Anderson LM, Chen CJ, et al. CYP2E1 genetic polymorphisms and risk of nasopharyngeal carcinoma in Taiwan. *J Natl Cancer Inst.* 1997;89:1207–1212.
37. Lin DX, Tang YM, Peng Q, Lu SX, Ambrosone CB, Kadlubar FF. Susceptibility to esophageal cancer and genetic polymorphisms in glutathione S-transferases T1, P1, and M1 and cytochrome P4502E1. *Cancer Epidemiol Biomarkers Prev.* 1998;7:1013–1018.
38. Katoh T, Kaneko S, Kohshi K, et al. Genetic polymorphisms of tobacco- and alcohol-related metabolizing enzymes and oral cavity cancer. *Int J Cancer.* 1999;83:606–609.
39. Watanabe J, Hayashi S, Kawajiri K. Different regulation and expression of the human CYP2E1 gene due to the RsaI polymorphism in the 5′-flanling region. *J Biochem.* 1994;116:321–326.
40. Carriere V, Berthou F, Baird S, Belloe C, Beaune P, de Waziers I. Human cytochrome P450 2E1 (CYP2E1): from genotype to phenotype. *Pharmacogenetics.* 1996;6:203–211.
41. Kim RB, O'Shea D, Wilkinson GR. Intraindividual variability of chlorzoxazone 6-hydroxylation in men and women and its relationship to CYP2E1 genetic polymorphisms. *Clin Phermacol Ther.* 1995;57:645–655.
42. Kim RB, Yamazaki H, Chiba K, et al. In vivo and in vitro characterization of CYP2E1 activity in Japanese and Caucasians. *J Pharmacol Exp Ther.* 1996;279:4–11.

British Journal of Cancer (2007), 1–8

www.bjcancer.com

Full Paper

The novel microtubule-interfering agent TZT-1027 enhances the anticancer effect of radiation *in vitro* and *in vivo*

Y Akashi[1], I Okamoto*[,1], M Suzuki[2], K Tamura[3], T Iwasa[1], S Hisada[4], T Satoh[1], K Nakagawa[1], K Ono[2] and M Fukuoka[1]

[1]Department of Medical Oncology, Kinki University School of Medicine, 377-2 Ohno-higashi, Osaka-Sayama, Osaka 589-8511, Japan; [2]Radiation Oncology Research Laboratory, Research Reactor Institute, Kyoto University, 2-1010 Asashiro-nishi, Kumatori-cho, Sennan-gun, Osaka 590-0494, Japan; [3]Department of Medical Oncology, Kinki University School of Medicine, Nara Hospital, 1248-1 Otodacho, Ikoma,Nara 630-0293, Japan; [4]Asuka Pharmaceutical Co. Ltd, 1604 Shimosakunobe, Takatu-ku, Kawasaki 213-8522, Japan

TZT-1027 is a novel anticancer agent that inhibits microtubule polymerisation and manifests potent antitumour activity in preclinical models. We have examined the effect of TZT-1027 on cell cycle progression as well as the anticancer activity of this drug both *in vitro* and *in vivo*. With the use of tsFT210 cells, which express a temperature-sensitive mutant of Cdc2, we found that TZT-1027 arrests cell cycle progression in mitosis, the phase of the cell cycle most sensitive to radiation. A clonogenic assay indeed revealed that TZT-1027 increased the sensitivity of H460 cells to γ-radiation, with a dose enhancement factor of 1.2. Furthermore, TZT-1027 increased the radiosensitivity of H460 and A549 cells in nude mice, as revealed by a marked delay in tumour growth and an enhancement factor of 3.0 and 2.2, respectively. TZT-1027 also potentiated the induction of apoptosis in H460 cells by radiation both *in vitro* and *in vivo*. Histological evaluation of H460 tumours revealed that TZT-1027 induced morphological damage to the vascular endothelium followed by extensive central tumour necrosis. Our results thus suggest that TZT-1027 enhances the antitumour effect of ionising radiation, and that this action is attributable in part to potentiation of apoptosis induction and to an antivascular effect. Combined treatment with TZT-1027 and radiation therefore warrants investigation in clinical trials as a potential anticancer strategy.
British Journal of Cancer advance online publication, 1 May 2007; doi:10.1038/sj.bjc.6603769 www.bjcancer.com

Keywords: TZT-1027; radiosensitisation; microtubule; mitotic arrest; apoptosis; antivascular effect

The combination of modalities of cancer treatment offers improvements in the survival of cancer patients compared with individual therapeutic approaches. Such therapeutic benefit has been achieved with combinations of chemo- and radiotherapy in a variety of cancers. The cytotoxicity of most chemotherapeutic agents as well as that of radiation is highly dependent on the phase of the cell cycle. Although various types of anticancer drugs are able to arrest cells at specific cell cycle checkpoints, the ability of antimicrotubule agents to block cell cycle progression in G_2-M phase is the biological basis for combination of these agents with radiation (Pawlik and Keyomarsi, 2004). Microtubule-interfering agents have been shown to increase the radiosensitivity of tumour cells in preclinical and clinical studies (Liebmann *et al*, 1994; Choy *et al*, 1995; Edelstein *et al*, 1996; Vokes *et al*, 1996; Kim *et al*, 2001, 2003; Hofstetter *et al*, 2005; Simoens *et al*, 2006).

TZT-1027 (Soblidotin), a novel microtubule-interfering agent synthesised from dolastatin 10 (Figure 1), exhibits greater antitumour activities and a reduced toxicity compared with its parent compound (Miyazaki *et al*, 1995). TZT-1027 inhibits microtubule assembly by binding to tubulin (Kobayashi *et al*, 1997; Natsume *et al*, 2000). *In vitro*, it inhibits the growth of various human cancer cells at low concentrations (Watanabe *et al*, 2000). *In vivo*, TZT-1027 also manifests a broad spectrum of activity against various murine tumours as well as human tumour xenografts, without inducing a pronounced reduction in body weight (Kobayashi *et al*, 1997; Watanabe *et al*, 2000, 2006a; Natsume *et al*, 2003, 2006). Furthermore, the drug exhibited a potent antivascular effect on existing vasculature in an advanced-stage tumour model (Otani *et al*, 2000). TZT-1027 is currently undergoing clinical evaluation, with a reduction in tumour size and disease stabilisation having been observed in a subset of patients (Schoffski *et al*, 2004; de Jonge *et al*, 2005; Greystoke *et al*, 2006; Tamura *et al*, 2007).

Despite its demonstrated efficacy against solid tumours, the effects of TZT-1027 in combination with radiation have not been examined. As an initial step in determining the antitumour activity of TZT-1027 in combination with radiation, we investigated the effect of this agent on cell cycle progression in synchronised tsFT210 cells (Osada *et al*, 1997), which harbour a temperature-sensitive mutant of Cdc2. We found that TZT-1027 induces arrest of cells in mitosis, the phase of the cell cycle most sensitive to radiation. We then studied the radiosensitising properties of TZT-1027 *in vitro* and *in vivo* with a human lung cancer model and elucidated the mechanism of radiosensitisation by this agent.

*Correspondence: Dr I Okamoto;
E-mail: okamoto@dotd.med.kindai.ac.jp
Revised 28 February 2007; accepted 2 April 2007

MATERIALS AND METHODS

Cell lines and reagents

tsFT210 mouse mammary carcinoma cells, which express a temperature-sensitive mutant of Cdc2, were kindly provided by H Kakeya (Antibiotics Laboratory, Discovery Research Institute, RIKEN, Saitama, Japan) and were maintained under a humidified atmosphere of 5% CO_2 in air at 32.0°C in RPMI 1640 (Sigma, St Louis, MO, USA) supplemented with 10% foetal bovine serum and 1% penicillin-streptomycin. H460 human lung large cell carcinoma and A549 human lung adenocarcinoma cells were obtained from American Type Culture Collection (Manassas, VA, USA) and were maintained as for tsFT210 cells with the exception that the culture temperature was 37°C. TZT-1027 (Figure 1) was provided by Daiichi Pharmaceutical Co. Ltd (Tokyo, Japan). Nocodazole and roscovitine were obtained from Sigma.

Cell cycle analysis

Cells were harvested, washed with phosphate-buffered saline (PBS), fixed with 70% methanol, washed again with PBS, and stained with propidium iodide (0.05 mg ml^{-1}) in a solution containing 0.1% Triton X-100, 0.1 mM EDTA, and RNase A (0.05 mg ml^{-1}). The stained cells ($\sim 1 \times 10^6$) were then analysed for DNA content with a flow cytometer (FACScalibur; Becton Dickinson, San Jose, CA, USA).

Measurement of mitotic index and apoptotic cells

Cells were harvested, washed with PBS, fixed with methanol : acetic acid (3 : 1, v/v), washed again with PBS, and stained with 4′,6-diamidino-2-phenylindole (DAPI) (0.5 μg ml^{-1}). The stained cells ($\sim 1 \times 10^6$) were observed with a fluorescence microscope (IX71; Olympus, Tokyo, Japan). To determine the proportion of mitotic or apoptotic cells, we scored at least 300 cells in each of at least three randomly selected microscopic fields for each of three slides per sample. Cells with condensed chromosomes and no obvious nuclear membrane were regarded as mitotic cells, and the mitotic index was calculated as the percentage of mitotic cells among total viable cells. Cells with fragmented and uniformly condensed nuclei were regarded as apoptotic cells.

Clonogenic assay

Exponentially growing H460 cells in 25-cm^2 flasks were harvested by exposure to trypsin and counted. They were diluted serially to appropriate densities and plated in triplicate in 25-cm^2 flasks containing 10 ml of medium. The cells were treated with 1 nM TZT-1027 or vehicle (dimethyl sulfoxide, or DMSO; final concentration, 0.1%) for 24 h and then exposed to various doses of γ-radiation with a ^{60}Co irradiator at a rate of ~ 0.82 Gy min^{-1} and at room temperature. The cells were then washed with PBS, cultured in drug-free medium for 10–14 days, fixed with methanol : acetic acid (10 : 1, v/v), and stained with crystal violet. Colonies containing >50 cells were counted. The surviving fraction was calculated as: (mean number of colonies)/(number of inoculated cells × plating efficiency). Plating efficiency was defined as the mean number of colonies divided by the number of inoculated cells for nonirradiated controls. The surviving fraction for combined treatment was corrected by that for TZT-1027 treatment alone. The dose enhancement factor (DEF) was calculated as the dose (Gy) of radiation that yielded a surviving fraction of 0.1 for vehicle-treated cells divided by that for TZT-1027-treated cells (after correction for drug toxicity).

In vivo antitumour activity of TZT-1027 with or without radiation

All animal studies were performed in accordance with the Recommendations for Handling of Laboratory Animals for Biomedical Research, compiled by the Committee on Safety and Ethical Handling Regulations for Laboratory Animal Experiments, Kyoto University. The ethical guidelines followed meet the requirements of the UKCCCR guidelines (Workman *et al*, 1998). Tumour cells (2×10^6) were injected subcutaneously into the right hind leg of 7-week-old female athymic nude mice. Tumour volume was determined from caliper measurement of tumour length (L) and width (W) according to the formula $LW^2/2$. Treatment was initiated when tumours in each group achieved an average volume of ~ 200–250 mm^3. Treatment groups consisted of control, TZT-1027 alone, radiation alone, and the combination of TZT-1027 and radiation. Each treatment group contained six to eight mice. TZT-1027 was administered intravenously in a single dose of 0.5 mg kg^{-1} of body weight; mice in the control and radiation-alone groups were injected with vehicle (physiological saline). Tumours in the leg were exposed to 10 Gy of γ-radiation with a ^{60}Co irradiator at a rate of ~ 0.32 Gy min^{-1} immediately after drug treatment. Growth delay (GD) was calculated as the time for treated tumours to achieve an average volume of 500 mm^3 minus the time for control tumours to reach 500 mm^3. The enhancement factor was then determined as: $(GD_{combination} - GD_{TZT-1027})/(GD_{radiation})$.

TUNEL staining

Mice were killed 14 days after treatment initiation and the tumours were removed and preserved in 10% paraformaldehyde. Apoptosis in tumour sections was determined by the terminal deoxynucleotidyl transferase-mediated dUTP-biotin nick-end labelling (TUNEL) assay with the use of an apoptosis detection kit (Chemicon, Temecula, CA, USA). The number of apoptotic cells was counted in 10 separate microscopic fields (× 100) for three sections of each tumour of each group.

Histological analysis

A single dose of TZT-1027 (2.0 mg kg^{-1}) or vehicle (physiological saline) was administered intravenously to mice when H460 tumours had achieved a volume of ~ 400 to 600 mm^3. Tumour tissue was extirpated 4 or 24 h after drug administration, and half of the tissue was fixed in 10% buffered formalin, embedded in paraffin, sectioned, and stained with hematoxylin-eosin. The other half of the tumour tissue was fixed for 12–48 h in zinc fixative

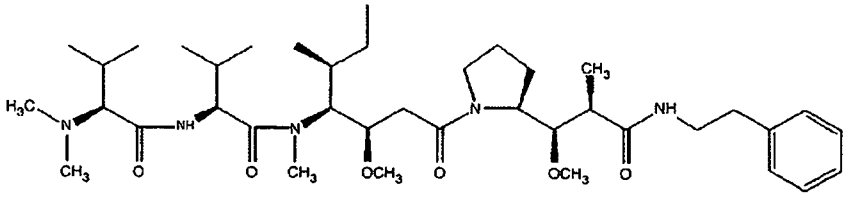

Figure 1 Chemical structure of TZT-1027.

(BD Biosciences, San Jose, CA, USA), embedded in paraffin, sectioned, and immunostained for CD31. Endogenous peroxidase activity was blocked by incubation of the latter sections for 20 min with 0.3% H_2O_2 in methanol, and nonspecific sites were blocked with antibody diluent (Dako Japan, Kyoto, Japan). Sections were then incubated overnight at 4°C with a 1:50 dilution of a rat monoclonal antibody to mouse CD31 (BD Biosciences), washed with PBS, and processed with a Histfine Simple Stain PO (M) kit (Nichirei, Tokyo, Japan) for detection of immune complexes. Sections were counterstained with Mayer's hematoxylin, covered with a coverslip with the use of a permanent mounting medium, and examined with a light microscope (CX41; Olympus, Tokyo, Japan).

Statistical analysis

Data are presented as means ± s.d. or s.e. and were compared by the unpaired Student's *t*-test. A P value of <0.05 was considered statistically significant.

RESULTS

Induction of cell cycle arrest at M phase but not at G_1-S in tsFT210 cells by TZT-1027

To examine the effect of TZT-1027 on cell cycle progression, we performed flow cytometric analysis of tsFT210 cells, which express a temperature-sensitive mutant of Cdc2. These mammary carcinoma cells exhibit a normal cell cycle distribution when incubated at the permissive temperature of 32.0°C, but they arrest at G_2 phase as a result of Cdc2 inactivation when incubated at the nonpermissive temperature of 39.4°C (Figure 2A and B). We synchronised tsFT210 cells at G_2 phase by incubation at 39.4°C for 17 h and then cultured them at 32.0°C for 6 h in the presence of nocodazole (an inhibitor of microtubule polymerisation), TZT-1027, or vehicle (DMSO). In the presence of vehicle alone, the number of cells in G_2 phase decreased markedly and there was a corresponding increase in the number of cells in G_1 phase, indicative of re-entry of cells into the cell cycle (Figure 2C). In contrast, treatment with nocodazole or TZT-1027 prevented the cells from passing through G_2-M phase (Figure 2D and E). Given that flow cytometric analysis did not distinguish between cells in M phase and those in G_2 phase, we determined the mitotic index of cells by DAPI staining and fluorescence microscopy. Most of the cells released from temperature-induced arrest in the presence of nocodazole manifested condensed chromosomes without a nuclear membrane, yielding a mitotic index of 93%; most of the cells had thus arrested in mitosis (Figure 2D). Most of the cells released from temperature-induced arrest in the presence of TZT-1027 showed similar mitotic figures, yielding a mitotic index of 85% (Figure 2E) and demonstrating that TZT-1027 also inhibits cell cycle progression at mitosis.

We next examined whether TZT-1027 affects the G_1-S transition. We arrested tsFT210 cells at G_2 phase by incubation at 39.4°C, released the cells into G_1 phase by shifting to the permissive temperature for 6 h, and then incubated them for an additional 6 h in the presence of roscovitine (an inhibitor of CDK2 that prevents cell cycle progression at G_1 phase), TZT-1027, or vehicle (Figure 3). The cells incubated with vehicle passed through G_1 phase and yielded a broad S-phase peak (Figure 3D), whereas those treated with roscovitine did not pass through G_1 phase (Figure 3E). In contrast, TZT-1027 had no effect on passage of the synchronised tsFT210 cells through the G_1-S transition (Figure 3F). Together,

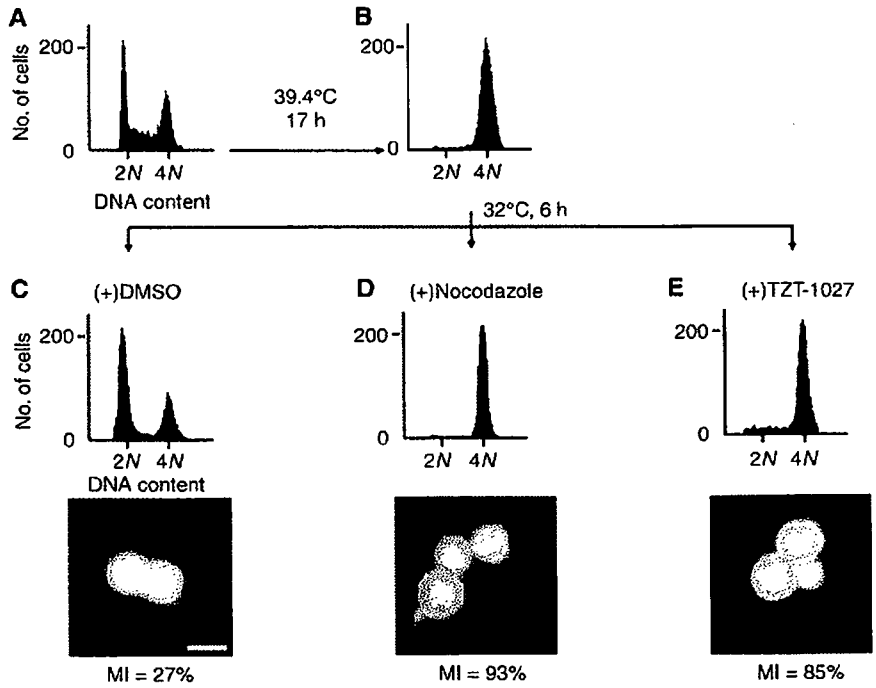

Figure 2 Inhibition of tsFT210 cell cycle progression through G_2-M by TZT-1027. Cells were cultured at the permissive temperature of 32.0°C (**A**) and then incubated for 17 h at the nonpermissive temperature of 39.4°C (**B**). They were subsequently released from G_2 arrest by incubation at 32.0°C for 6 h in the presence of DMSO (**C**), 1 μM nocodazole (**D**), or 2 nM TZT-1027 (**E**). At each stage of the protocol, cells were analysed for DNA content by staining with propidium iodide and flow cytometry. The 2N and 4N peaks indicate cells in G_0-G_1 and G_2-M phases of the cell cycle, respectively. The cells were also stained with DAPI and examined by fluorescence microscopy after treatment with DMSO, nocodazole, or TZT-1027 (lower panels), and the mitotic index (MI) was determined; scale bar, 20 μm. Data are representative of at least three independent experiments.

these results indicate that the effect of TZT-1027 on cell cycle progression is specific to M phase.

Induction of cell cycle arrest at M phase in asynchronous H460 cells by TZT-1027

We next examined whether TZT-1027 induced mitotic arrest in asynchronous H460 human non-small cell lung cancer cells. Flow cytometric analysis revealed that treatment of H460 cells with TZT-1027 for 24 h induced a threefold increase in the proportion of cells with a DNA content of 4N compared with that apparent for vehicle-treated cells (29.1 *vs* 8.7%) (Figure 4A and B). Furthermore, DAPI staining revealed that TZT-1027 induced a significant increase in the mitotic index of H460 cells compared with that for the control cells (23.3 *vs* 4.6%) (Figure 4C and D), indicating that most of the TZT-1027-treated cells with a DNA content of 4N were arrested in M phase rather than in G_2 phase. These observations thus showed that TZT-1027 also induced mitotic arrest in asynchronous H460 cells.

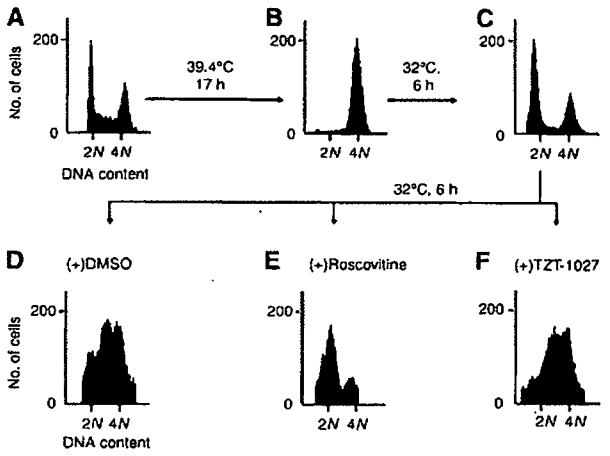

Figure 3 Lack of effect of TZT-1027 on tsFT210 cell cycle progression through G_1-S. Exponentially growing tsFT210 cells (**A**) were arrested in G_2 phase by incubation for 17 h at 39.4°C (**B**). The cells were incubated at 32.0°C first for 6 h to allow progression to G_1 phase (**C**) and then for an additional 6 h in the presence of DMSO (**D**), 50 μM roscovitine (**E**), or 2 nM TZT-1027 (**F**). At each stage of the protocol, cells were analysed for DNA content by flow cytometry. Data are representative of at least three independent experiments.

Radiosensitisation of H460 cells by TZT-1027 *in vitro*

Cells in M phase are more sensitive to radiation than are those in other phases of the cell cycle. Given that exposure of H460 cells to TZT-1027-induced mitotic arrest, we next examined whether this agent might sensitise H460 cells to γ-radiation with the use of a clonogenic assay. H460 cells were incubated for 24 h with 1 nM TZT-1027 or vehicle (DMSO) and then exposed to various doses (0, 2, 4, or 6 Gy) of γ-radiation. The cells were then allowed to form colonies in drug-free medium for 10–14 days. Survival curves revealed that TZT-1027 increased the radiosensitivity of H460 cells, with a DEF of 1.2 (Figure 5A).

To determine whether radiosensitisation by TZT-1027 was reflected by an increase in the proportion of apoptotic cells, we exposed H460 cells to 1 nM TZT-1027 or vehicle for 24 h, treated the cells with various doses (0, 2, 4, or 6 Gy) of radiation, and then incubated them in drug-free medium for an additional 24 h before quantification of apoptosis. Combined treatment with TZT-1027 and 4 or 6 Gy of radiation resulted in a significant increase in the number of apoptotic cells compared with the sum of the values for treatment with drug alone or radiation alone (Figure 5B). TZT-1027 thus promoted radiation-induced apoptosis in H460 cells.

Radiosensitisation of H460 cells and A549 cells by TZT-1027 *in vivo*

To determine whether the TZT-1027-induced increase in the radiosensitivity of tumour cells observed *in vitro* might also be apparent *in vivo*, we injected H460 cells or A549 human lung

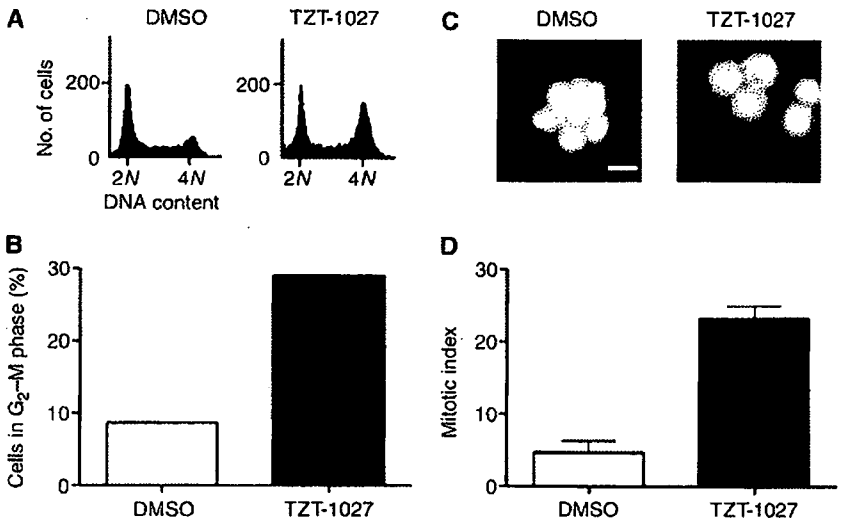

Figure 4 Induction of cell cycle arrest at M phase in H460 cells by TZT-1027. H460 cells were incubated in the presence of 1 nM TZT-1027 or vehicle (DMSO) for 24 h, after which DNA content was measured by flow cytometry (**A**) and the fraction of cells in G_2-M phase was determined (**B**). The cells were also stained with DAPI and examined by fluorescence microscopy (**C**) and the mitotic index was determined (**D**). Data in (**A**) through (**C**) are representative of at least three independent experiments; data in (**D**) are means ± s.d. of values from three independent experiments. Scale bar in (**C**), 20 μm.

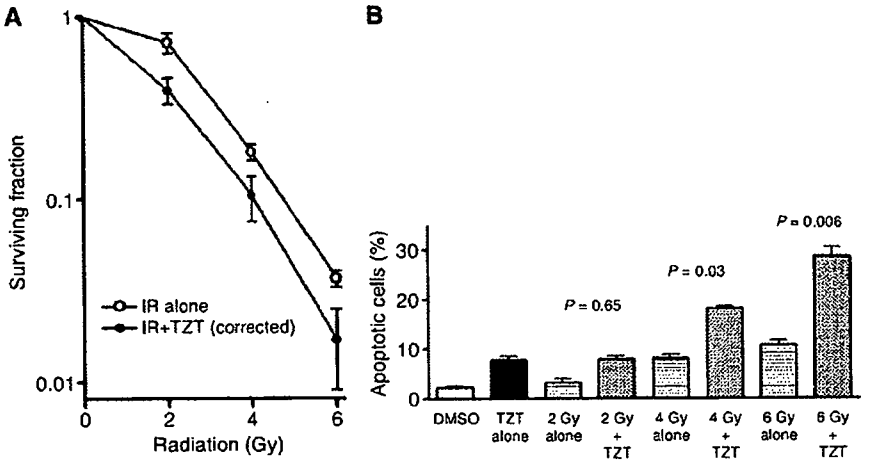

Figure 5 Sensitisation of H460 cells to γ-radiation by TZT-1027 *in vitro*. (**A**) Clonogenic assay. Cells were incubated with 1 nM TZT-1027 or vehicle (DMSO) for 24 h, exposed to the indicated doses of γ-radiation, and then incubated in drug-free medium for 10–14 days for determination of colony-forming ability. Survival curves were generated after correction of colony formation observed for combined treatment with ionising radiation (IR) and TZT-1027 by that apparent for treatment with TZT-1027 alone. (**B**) Assay of apoptosis. Cells were incubated with 1 nM TZT-1027 or vehicle (DMSO) for 24 h, exposed to various doses (0, 2, 4, or 6 Gy) of γ-radiation, and then incubated for 24 h in drug-free medium. Cells were then fixed and stained with DAPI for determination of the proportion of apoptotic cells by fluorescence microscopy. Data in (**A**) and (**B**) are means ± s.d. of values from three independent experiments. *P* values in (**B**) are for comparison of the value for combined treatment with TZT-1027 and radiation vs the sum of the corresponding values for each treatment alone, after correction of all data by the control (DMSO) value.

adenocarcinoma cells into nude mice in order to elicit the formation of solid tumours. The mice were then treated with TZT-1027, radiation, or both modalities. Treatment with TZT-1027 alone (single dose of 0.5 mg kg^{-1}) or with radiation alone (single dose of 10 Gy) resulted in relatively small inhibitory effects on tumour growth, whereas combined treatment with both TZT-1027 and radiation exerted a markedly greater inhibitory effect (Figure 6A and B). The tumour GDs induced by treatment with TZT-1027 alone, radiation alone, or both TZT-1027 and radiation were 1.0, 2.6, and 8.8 days, respectively, for H460 cells and 1.4, 4.9, and 12.4 days, respectively, for A549 cells (Table 1). The enhancement factor for the effect of TZT-1027 on the efficacy of radiation was 3.0 for H460 cells and 2.2 for A549 cells, revealing the effect to be greater than additive. No pronounced tissue damage or toxicities such as diarrhoea or weight loss of >10% were observed in mice in any of the four treatment groups (Table 2).

We examined the effects of the treatment protocols on apoptosis in H460 tumours by TUNEL staining of tumour sections. Quantification of the number of apoptotic cells revealed that the combined treatment with radiation and TZT-1027 induced a significant increase in this parameter compared with treatment with radiation or TZT-1027 alone (Figure 6C).

Histological appearance of H460 tumours after administration of TZT-1027

Finally, we examined whether an effect of TZT-1027 on tumour vasculature might contribute to the antitumour activity of this drug *in vivo*. Mice harbouring H460 tumours were injected with TZT-1027, and the tumours were excised 4 or 24 h thereafter and examined by hematoxylin-eosin staining (Figure 7A–C) or by immunostaining for the endothelial cell marker CD31 (Figure 7D and E). Tumour capillaries appeared congested, with thrombus formation, and showed a loss of endothelial cells 4 h after administration of TZT-1027 (Figure 7B and E), whereas vessels within viable areas of control tumours were generally not congested and showed an intact normal endothelium (Figure 7A and D). The effects of TZT-1027 on the tumour vasculature appeared selective, given that neither loss of CD31 staining nor vessel congestion was apparent in the vasculature of surrounding normal tissue after drug treatment (Figure 7E). Extensive necrosis was apparent at the tumour core, with a characteristic thin rim of viable tumour cells remaining at the periphery, 24 h after TZT-1027 administration (Figure 7C). These results were thus indicative of a characteristic antivascular effect of TZT-1027 in the H460 tumour model.

DISCUSSION

TZT-1027 is a novel antitumour agent that inhibits microtubule polymerisation and exhibits potent antitumour activity in preclinical models (Miyazaki *et al*, 1995; Kobayashi *et al*, 1997; Natsume *et al*, 2000, 2003, 2006; Otani *et al*, 2000; Watanabe *et al*, 2000, 2006a). We investigated the effect of TZT-1027 on cell cycle progression with the use of tsFT210 cells, which can be synchronised in G_2 phase by incubation at 39.4°C and consequent inactivation of Cdc2 (Osada *et al*, 1997; Tamura *et al*, 1999). The use of these cells allows cell synchronisation without the need for agents that prevent DNA synthesis (such as hydroxyurea or thymidine) or that inhibit formation of the mitotic spindle (such as nocodazole). Although such agents halt cell cycle progression in specific phases of the cycle, they are also toxic and kill a proportion of the treated cells. The tsFT210 cell system is thus suited to sensitive analysis of the effects of new compounds on cell cycle progression without loss of cell viability. We have now shown that tsFT210 cells released from G_2 arrest by incubation at 32.0°C failed to pass through M phase in the presence of TZT-1027. Although previous flow cytometric analysis of exponentially growing tumour cells revealed that TZT-1027 induced a marked increase in the proportion of cells in G_2-M (Watanabe *et al*, 2000), it was uncertain whether the drug arrested cell cycle progression in G_2 or in mitosis. Our morphological data now indicate that, similar to the effect of nocodazole, TZT-1027 arrested tsFT210 cells in M phase rather than in G_2, consistent with the mode of action of this new compound. Given that microtubules contribute to various cellular functions in addition to cell division, including intracellular transport and signal transduction (Mollinedo and Gajate,

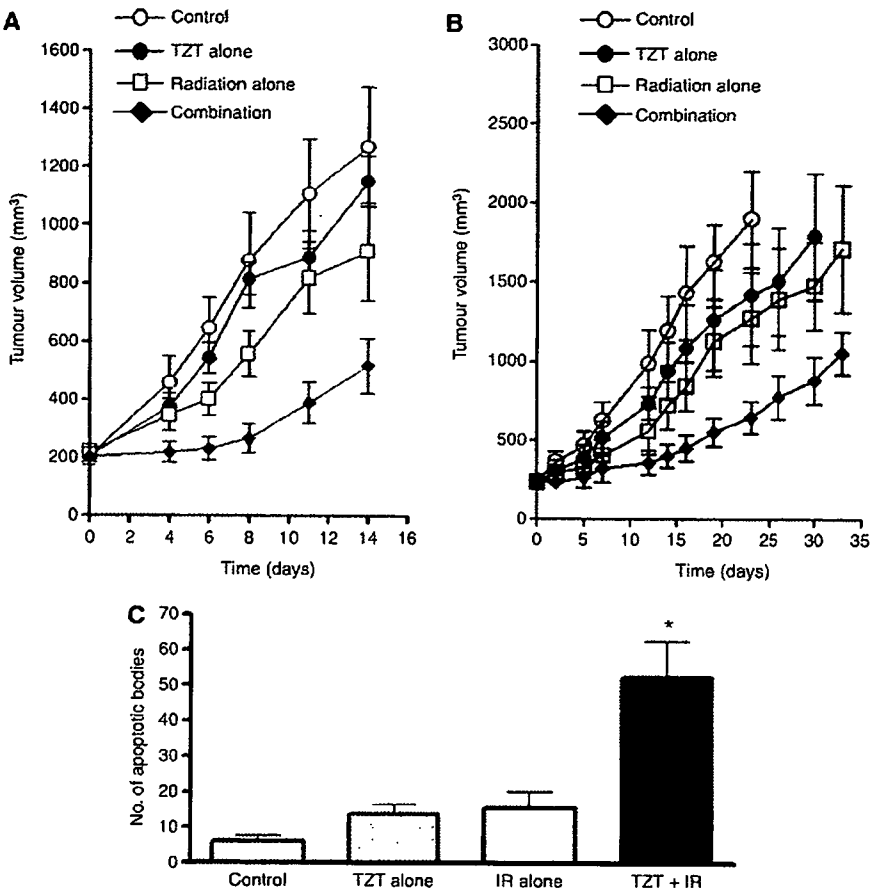

Figure 6 Sensitisation of H460 and A549 cells to γ-radiation by TZT-1027 *in vivo*. (**A** and **B**) Evaluation of tumour growth. Nude mice with H460 (**A**) or A549 (**B**) tumour xenografts (~200 to 250 mm^3) were treated with a single intravenous dose of TZT-1027 (0.5 mg kg^{-1}), a single dose of γ-radiation (10 Gy), or neither (control) or both modalities, and tumour volume was determined at the indicated times thereafter. Data are means ± s.e. for six to eight mice per group. (**C**) Quantification of apoptotic cells in H460 tumour sections by TUNEL staining 14 days after the initiation of treatment as in (**A**). Data are means ± s.d. $^*P<0.05$ *vs* mice treated with TZT-1027 alone or radiation alone.

Table 1 Tumour growth delay value

	H460		A549	
Treatment	**Days[a]**	**GD[b]**	**Days**	**GD**
Control	4.5		5.5	
TZT-1027 alone	5.5	1	6.9	1.4
Radiation alone	7.1	2.6	10.4	4.9
TZT-1027 + Radiation	13.3	8.8	17.9	12.4
Enhancement factor	3		2.2	

[a]Days, the period needed for the sizes of xenografts in each group to reach 500 mm^3; [b]GD, the additional periods needed for the sizes of xenografts in each group to reach 500 mm^3 in addition to the period needed for controls to reach 500 mm^3.

Table 2 Body weight loss

	% of B.W.L[a]	
	H460	**A549**
Control	3.6	1.2
TZT-1027 alone	9.9	5.2
Radiation alone	9.7	5.5
TZT-1027+Radiation	8.7	9.9

[a]% of B.W.L, relative body weight loss 7 days after the initiation of the treatment.

2003), TZT-1027 might also be expected to affect tumour cells in interphase. With the use of synchronised tsFT210 cells, however, we found that TZT-1027 had no effect on progression of cells through the G_1–S transition of the cell cycle. The effect of TZT-1027 on cell cycle progression thus appears to be specific to M phase.

Given that cells are most sensitive to radiation during mitosis (Sinclair and Morton, 1966; Sinclair, 1968; Pawlik and Keyomarsi, 2004), we next investigated the possible interaction between TZT-1027 and ionising radiation in human lung cancer cell lines. We found that TZT-1027 increased the sensitivity of H460 cells to γ-radiation *in vitro*. The proportion of H460 cells in mitotic phase at the time of irradiation was increased by TZT-1027 treatment, consistent with the notion that this effect contributes to the observed radiosensitisation induced by this drug. TZT-1027 was previously shown to induce apoptosis in several tumour cell lines (Watanabe *et al*, 2000). Although the relation between apoptosis and radiosensitivity is controversial (Lawrence *et al*, 2001; Pawlik and Keyomarsi, 2004), we showed that treatment of H460 cells with

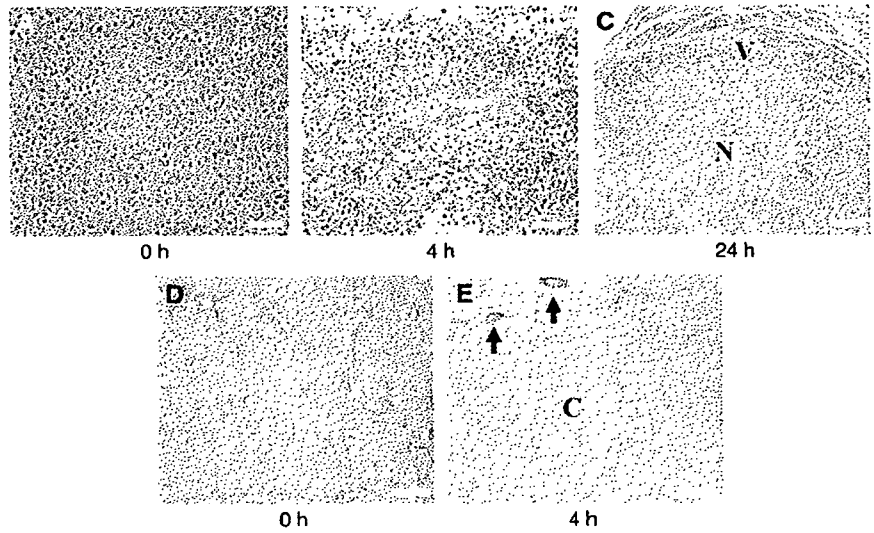

Figure 7 Histological analysis of H460 tumours after treatment with TZT-1027. Mice bearing H460 tumour xenografts were treated with a single dose of TZT-1027 (2.0 mg kg^{-1}), and the tumours were excised at various times thereafter and either stained with hematoxylin-eosin (**A**–**C**) or immunostained for CD31 (**D** and **E**). (**A** and **D**) Control sections of an untreated tumour showing normal capillaries with an intact endothelium and viable tumour cells. (**B** and **E**) Sections of a tumour removed 4 h after administration of TZT-1027. Vascular congestion, with pink deposits of fibrin, and loss of endothelial cells as well as diffuse tumour cell degeneration are apparent in (**b**). Dark immunostaining of intact endothelium (arrows) is apparent in surrounding normal connective tissue, whereas little staining of endothelial cells was observed in the core (**C**) of the tumour (**E**). (**C**) Section of a tumour removed 24 h after TZT-1027 administration, showing extensive central necrosis (N) and a rim of viable cells (V). Scale bars: 50 μm (**A** and **B**), 100 μm (**C**), and 200 μm (**D** and **E**).

TZT-1027 before irradiation induced a marked increase in the proportion of apoptotic cells compared with that apparent with radiation alone. These results thus suggested that potentiation of apoptosis contributed to radiosensitisation by TZT-1027.

Combined treatment with radiation and a single administration of TZT-1027 also inhibited the growth of tumours formed by H460 or A549 cells *in vivo* to a greater extent than did either treatment alone. Tumour microenvironmental factors, such as the vascular supply, are important determinants of sensitivity to radiation therapy *in vivo*. The ability of microtubule-targeting agents to induce a rapid shutdown of the existing tumour vasculature has been recognised by their designation as vascular-targeting agents (VTAs) (Jordan and Wilson, 2004). Treatment with VTAs such as ZD6126 and combretastatin A-4-P typically results in the destruction of large areas of a tumour, with surviving cells remaining only at the tumour periphery (Dark *et al*, 1997; Blakey *et al*, 2002). These peripheral viable tumour cells presumably derive their nutritional support from nearby normal blood vessels that are not responsive to VTA treatment (Li *et al*, 1998; Siemann and Rojiani, 2002). Such support together with a rapid upregulation of angiogenic factors such as vascular endothelial growth factor may directly facilitate the growth and expansion of the remaining tumour cells (Wachsberger *et al*, 2003; Thorpe, 2004). Given that these residual tumour cells are likely well oxygenated (Wachsberger *et al*, 2003), they are an ideal target for radiation therapy. Several studies have recently shown that treatment with VTAs enhances the therapeutic effect of radiotherapy (Li *et al*, 1998; Siemann and Rojiani, 2002, 2005; Horsman and Murata, 2003; Masunaga *et al*, 2004), consistent with the idea that the components of such combination therapy act in a complementary manner, with VTAs attacking the poorly oxygenated cell population in the central region of tumours and radiation killing the well-oxygenated proliferating cells at the tumour periphery (Li *et al*, 1998; Siemann and Rojiani, 2002; Wachsberger *et al*, 2003). TZT-1027 was previously shown to increase vascular permeability and to induce a decrease in tumour blood flow followed by a marked increase in tissue necrosis in the central region of tumour xenografts (Otani *et al*, 2000; Watanabe *et al*, 2006b). We have now shown that TZT-1027 treatment resulted in congestion and occlusion of tumour blood vessels followed by extensive necrosis of the tumour core, with only a thin rim of viable tumour cells remaining, in the H460 tumour model, suggesting that TZT-1027 acts as a VTA. The action of TZT-1027 as a VTA might thus contribute to the radiosensitising effect observed *in vivo* in the present study.

The clinical use of microtubule-interfering agents such as taxanes in combination with radiation has been successful in improving local tumour control. However, taxanes are often of limited efficacy because of the development of cellular resistance such as that mediated by P-glycoprotein-dependent drug efflux (Goodin *et al*, 2004). The action of TZT-1027 has been suggested to be less affected by multidrug resistance factors, including overexpression of P-glycoprotein, than that of other tubulin inhibitors (Watanabe *et al*, 2006a), suggesting that TZT-1027 may be effective in the treatment of taxane-refractory tumours. Further investigations are thus warranted to examine the combined effects of TZT-1027 and ionising radiation on drug-resistant tumour cells. Whether TZT-1027 enhances the tumour response to clinically relevant fractionated doses of radiation such as 2 Gy per fraction also warrants further study.

In conclusion, we have found that the inhibitory effect of TZT-1027 on cell cycle progression is highly specific to M phase. Moreover, TZT-1027 enhanced the effects of radiation on human cancer cells both *in vitro* and in animal models *in vivo*. These preclinical results provide a rationale for future clinical investigations of the therapeutic efficacy of TZT-1027 in combination with radiotherapy.

ACKNOWLEDGEMENTS

We thank H Kakeya for providing tsFT210 cells as well as M Kobayashi, T Natsume, E Hatashita, Y Yamada, and S Ono for technical assistance.

REFERENCES

Blakey DC, Westwood FR, Walker M, Hughes GD, Davis PD, Ashton SE, Ryan AJ (2002) Antitumor activity of the novel vascular targeting agent ZD6126 in a panel of tumor models. *Clin Cancer Res* 8: 1974–1983

Choy H, Yee L, Cole BF (1995) Combined-modality therapy for advanced non-small cell lung cancer: paclitaxel and thoracic irradiation. *Semin Oncol* 22: 38–44

Dark GG, Hill SA, Prise VE, Tozer GM, Pettit GR, Chaplin DJ (1997) Combretastatin A-4, an agent that displays potent and selective toxicity toward tumor vasculature. *Cancer Res* 57: 1829–1834

de Jonge MJ, van der Gaast A, Planting AS, van Doorn L, Lems A, Boot I, Wanders J, Satomi M, Verweij J (2005) Phase I and pharmacokinetic study of the dolastatin 10 analogue TZT-1027, given on days 1 and 8 of a 3-week cycle in patients with advanced solid tumors. *Clin Cancer Res* 11: 3806–3813

Edelstein MP, Wolfe III LA, Duch DS (1996) Potentiation of radiation therapy by vinorelbine (Navelbine) in non-small cell lung cancer. *Semin Oncol* 23: 41–47

Goodin S, Kane MP, Rubin EH (2004) Epothilones: mechanism of action and biologic activity. *J Clin Oncol* 22: 2015–2025

Greystoke A, Blagden S, Thomas AL, Scott E, Attard G, Molife R, Vidal L, Pacey S, Sarkar D, Jenner A, De-Bono JS, Steward W (2006) A phase I study of intravenous TZT-1027 administered on day 1 and day 8 of a three-weekly cycle in combination with carboplatin given on day 1 alone in patients with advanced solid tumours. *Ann Oncol* 17: 1313–1319

Hofstetter B, Vuong V, Broggini-Tenzer A, Bodis S, Ciernik IF, Fabbro D, Wartmann M, Folkers G, Pruschy M (2005) Patupilone acts as radiosensitizing agent in multidrug-resistant cancer cells *in vitro* and *in vivo*. *Clin Cancer Res* 11: 1588–1596

Horsman MR, Murata R (2003) Vascular targeting effects of ZD6126 in a C3H mouse mammary carcinoma and the enhancement of radiation response. *Int J Radiat Oncol Biol Phys* 57: 1047–1055

Jordan MA, Wilson L (2004) Microtubules as a target for anticancer drugs. *Nat Rev Cancer* 4: 253–265

Kim JC, Kim JS, Saha D, Cao Q, Shyr Y, Choy H (2003) Potential radiation-sensitizing effect of semisynthetic epothilone B in human lung cancer cells. *Radiother Oncol* 68: 305–313

Kim JS, Amorino GP, Pyo H, Cao Q, Price JO, Choy H (2001) The novel taxane analogs, BMS-184476 and BMS-188797, potentiate the effects of radiation therapy *in vitro* and *in vivo* against human lung cancer cells. *Int J Radiat Oncol Biol Phys* 51: 525–534

Kobayashi M, Natsume T, Tamaoki S, Watanabe J, Asano H, Mikami T, Miyasaka K, Miyazaki K, Gondo M, Sakakibara K, Tsukagoshi S (1997) Antitumor activity of TZT-1027, a novel dolastatin 10 derivative. *Jpn J Cancer Res* 88: 316–327

Lawrence TS, Davis MA, Hough A, Rehemtulla A (2001) The role of apoptosis in 2′,2′-difluoro-2′-deoxycytidine (gemcitabine)-mediated radiosensitization. *Clin Cancer Res* 7: 314–319

Li L, Rojiani A, Siemann DW (1998) Targeting the tumor vasculature with combretastatin A-4 disodium phosphate: effects on radiation therapy. *Int J Radiat Oncol Biol Phys* 42: 899–903

Liebmann J, Cook JA, Fisher J, Teague D, Mitchell JB (1994) *In vitro* studies of Taxol as a radiation sensitizer in human tumor cells. *J Natl Cancer Inst* 86: 441–446

Masunaga S, Sakurai Y, Suzuki M, Nagata K, Maruhashi A, Kinash Y, Ono K (2004) Combination of the vascular targeting agent ZD6126 with boron neutron capture therapy. *Int J Radiat Oncol Biol Phys* 60: 920–927

Miyazaki K, Kobayashi M, Natsume T, Gondo M, Mikami T, Sakakibara K, Tsukagoshi S (1995) Synthesis and antitumor activity of novel dolastatin 10 analogs. *Chem Pharm Bull (Tokyo)* 43: 1706–1718

Mollinedo F, Gajate C (2003) Microtubules, microtubule-interfering agents and apoptosis. *Apoptosis* 8: 413–450

Natsume T, Watanabe J, Horiuchi T, Kobayashi M (2006) Combination effect of TZT-1027 (Soblidotin) with other anticancer drugs. *Anticancer Res* 26: 1145–1151

Natsume T, Watanabe J, Koh Y, Fujio N, Ohe Y, Horiuchi T, Saijo N, Nishio K, Kobayashi M (2003) Antitumor activity of TZT-1027 (Soblidotin) against vascular endothelial growth factor-secreting human lung cancer *in vivo*. *Cancer Sci* 94: 826–833

Natsume T, Watanabe J, Tamaoki S, Fujio N, Miyasaka K, Kobayashi M (2000) Characterization of the interaction of TZT-1027, a potent antitumor agent, with tubulin. *Jpn J Cancer Res* 91: 737–747

Osada H, Cui CB, Onose R, Hanaoka F (1997) Screening of cell cycle inhibitors from microbial metabolites by a bioassay using a mouse cdc2 mutant cell line, tsFT210. *Bioorg Med Chem* 5: 193–203

Otani M, Natsume T, Watanabe JI, Kobayashi M, Murakoshi M, Mikami T, Nakayama T (2000) TZT-1027, an antimicrotubule agent, attacks tumor vasculature and induces tumor cell death. *Jpn J Cancer Res* 91: 837–844

Pawlik TM, Keyomarsi K (2004) Role of cell cycle in mediating sensitivity to radiotherapy. *Int J Radiat Oncol Biol Phys* 59: 928–942

Schoffski P, Thate B, Beutel G, Bolte O, Otto D, Hofmann M, Ganser A, Jenner A, Cheverton P, Wanders J, Oguma T, Atsumi R, Satomi M (2004) Phase I and pharmacokinetic study of TZT-1027, a novel synthetic dolastatin 10 derivative, administered as a 1-hour intravenous infusion every 3 weeks in patients with advanced refractory cancer. *Ann Oncol* 15: 671–679

Siemann DW, Rojiani AM (2002) Enhancement of radiation therapy by the novel vascular targeting agent ZD6126. *Int J Radiat Oncol Biol Phys* 53: 164–171

Siemann DW, Rojiani AM (2005) The vascular disrupting agent ZD6126 shows increased antitumor efficacy and enhanced radiation response in large, advanced tumors. *Int J Radiat Oncol Biol Phys* 62: 846–853

Simoens C, Vermorken JB, Korst AE, Pauwels B, De Pooter CM, Pattyn GG, Lambrechts HA, Breillout F, Lardon F (2006) Cell cycle effects of vinflunine, the most recent promising Vinca alkaloid, and its interaction with radiation, *in vitro*. *Cancer Chemother Pharmacol* 58: 210–218

Sinclair WK (1968) Cyclic x-ray responses in mammalian cells *in vitro*. *Radiat Res* 33: 620–643

Sinclair WK, Morton RA (1966) X-ray sensitivity during the cell generation cycle of cultured Chinese hamster cells. *Radiat Res* 29: 450–474

Tamura K, Nakagawa K, Kurata T, Satoh T, Nogami T, Takeda K, Mitsuoka S, Yoshimura N, Kudoh S, Negoro S, Fukuoka M (2007) Phase I study of TZT-1027, a novel synthetic dolastatin 10 derivative and inhibitor of tubulin polymerization, which was administered to patients with advanced solid tumors on days 1 and 8 in 3-week courses. *Cancer Chemother Pharmacol* (in press)

Tamura K, Rice RL, Wipf P, Lazo JS (1999) Dual G_1 and G_2/M phase inhibition by SC-alpha alpha delta 9, a combinatorially derived Cdc25 phosphatase inhibitor. *Oncogene* 18: 6989–6996

Thorpe PE (2004) Vascular targeting agents as cancer therapeutics. *Clin Cancer Res* 10: 415–427

Vokes EE, Haraf DJ, Masters GA, Hoffman PC, Drinkard LC, Ferguson M, Olak J, Watson S, Golomb HM (1996) Vinorelbine (Navelbine), cisplatin, and concomitant radiation therapy for advanced malignancies of the chest: a Phase I study. *Semin Oncol* 23: 48–52

Wachsberger P, Burd R, Dicker AP (2003) Tumor response to ionizing radiation combined with antiangiogenesis or vascular targeting agents: exploring mechanisms of interaction. *Clin Cancer Res* 9: 1957–1971

Watanabe J, Minami M, Kobayashi M, Natsume T, Watanabe J, Horiuchi T, Kobayashi M (2006a) Antitumor activity of TZT-1027 (Soblidotin). *Anticancer Res* 26: 1973–1981

Watanabe J, Natsume T, Fujio N, Miyasaka K, Kobayashi M (2000) Induction of apoptosis in human cancer cells by TZT-1027, an antimicrotubule agent. *Apoptosis* 5: 345–353

Watanabe J, Natsume T, Kobayashi M (2006b) Antivascular effects of TZT-1027 (Soblidotin) on murine Colon26 adenocarcinoma. *Cancer Sci* 97: 1410–1416

Workman P, Twentyman P, Balkwill F, Balmain A, Chaplin D, Double J, Embleton J, Newell D, Raymond R, Stables J, Stephens T, Wallace J (1998) United Kingdom Co-ordinating Committee on Cancer Research (UKCCCR) Guidelines for the Welfare of Animals in Experimental Neoplasia 2nd edn. *Br J Cancer* 77: 1–10

British Journal of Cancer (2008), 1–7

www.bjcancer.com

Full Paper

Enhancement of the antitumor activity of ionising radiation by nimotuzumab, a humanised monoclonal antibody to the epidermal growth factor receptor, in non-small cell lung cancer cell lines of differing epidermal growth factor receptor status

Y Akashi[1], I Okamoto*[,1], T Iwasa[1], T Yoshida[1], M Suzuki[2], E Hatashita[1], Y Yamada[1], T Satoh[1], M Fukuoka[1], K Ono[2] and K Nakagawa[1]

[1]*Department of Medical Oncology, Kinki University School of Medicine, 377-2 Ohno-higashi, Osaka-Sayama, Osaka 589-8511, Japan;* [2]*Radiation Oncology Research Laboratory, Research Reactor Institute, Kyoto University, 2-1010 Asashiro-nishi, Kumatori-cho, Sennan-gun, Osaka 590-0494, Japan*

The expression and activity of the epidermal growth factor receptor (EGFR) are determinants of radiosensitivity in several tumour types, including non-small cell lung cancer (NSCLC). However, little is known of whether genetic alterations of *EGFR* in NSCLC cells affect the therapeutic response to monoclonal antibodies (mAbs) to EGFR in combination with radiation. We examined the effects of nimotuzumab, a humanised mAb to EGFR, in combination with ionising radiation on human NSCLC cell lines of differing *EGFR* status. Flow cytometry revealed that H292 and Ma-1 cells expressed high and moderate levels of EGFR on the cell surface, respectively, whereas H460, H1299, and H1975 cells showed a low level of surface EGFR expression. Immunoblot analysis revealed that EGFR phosphorylation was inhibited by nimotuzumab in H292 and Ma-1 cells but not in H460, H1299, or H1975 cells. Nimotuzumab augmented the cytotoxic effect of radiation in H292 and Ma-1 cells in a clonogenic assay *in vitro*, with a dose enhancement factor of 1.5 and 1.3, respectively. It also enhanced the antitumor effect of radiation on H292 and Ma-1 cell xenografts in nude mice, with an enhancement factor of 1.3 and 4.0, respectively. Nimotuzumab did not affect the radioresponse of H460 cells *in vitro* or *in vivo*. Nimotuzumab enhanced the antitumor efficacy of radiation in certain human NSCLC cell lines *in vitro* and *in vivo*. This effect may be related to the level of EGFR expression on the cell surface rather than to *EGFR* mutation.
British Journal of Cancer advance online publication, 5 February 2008; doi:10.1038/sj.bjc.6604222 www.bjcancer.com

Keywords: epidermal growth factor receptor; non-small cell lung cancer; nimotuzumab; monoclonal antibody; genetic alteration; radiosensitisation

Epidermal growth factor receptor (EGFR) is a receptor tyrosine kinase that is abnormally upregulated and activated in a variety of tumours (Baselga, 2002). Deregulation of receptor tyrosine kinases as a result of overexpression or activating mutations is frequently associated with human cancers and leads to the promotion of cell proliferation or migration, inhibition of cell death, or the induction of angiogenesis (Gschwind *et al*, 2004). The epidermal growth factor receptor has thus been identified as an important target in cancer therapy (Baselga and Arteaga, 2005). Several agents, including small-molecule inhibitors of the tyrosine kinase activity of EGFR (EGFR-TKIs) and monoclonal antibodies (mAbs) specific for EGFR, have been designed to block EGFR signalling selectively (Ettinger, 2006; Harari and Huang, 2006; Imai and Takaoka, 2006). Among EGFR-TKIs, gefitinib and erlotinib have been extensively evaluated in non-small cell lung cancer (NSCLC), and sensitivity to these drugs has been associated with the presence of somatic mutations in the EGFR kinase domain or with *EGFR* amplification (Lynch *et al*, 2004; Paez *et al*, 2004; Pao *et al*, 2004; Cappuzzo *et al*, 2005; Mitsudomi *et al*, 2005; Takano *et al*, 2005). Various mAbs to EGFR are also undergoing preclinical and clinical trials of their efficacy as anticancer agents. However, biological markers able to predict the response to such antibodies have remained elusive.

The possibility of combining chemotherapy or radiation therapy with anti-EGFR mAb treatment has generated much interest, because the cellular targets for these agents and their mechanisms of action are different (Baumann and Krause, 2004). Studies have thus been undertaken to determine whether inhibition of EGFR signalling improves the response to chemotherapy or radiation therapy. Preclinical studies have shown that the anti-EGFR mAb cetuximab markedly increases the cytotoxic effect of chemotherapy or radiation therapy in various EGFR-expressing tumour cell lines (Huang *et al*, 1999; Milas *et al*, 2000; Buchsbaum *et al*, 2002; Prewett *et al*, 2002; Raben *et al*, 2005; Ettinger, 2006). A phase III clinical trial also showed that the combination of cetuximab with

*Correspondence: Dr I Okamoto;
E-mail: chi-okamoto@dotd.med.kindai.ac.jp
Revised 20 November 2007; accepted 7 January 2008

radiation therapy resulted in a significant improvement in local control and survival compared with radiation therapy alone, without an increase in radiation-induced side effects, in patients with locally advanced head and neck cancer (Bonner *et al*, 2006).

Nimotuzumab (also known as h-R3) is a humanised anti-EGFR mAb, which is currently undergoing clinical evaluation. In a preclinical study, nimotuzumab showed marked antiproliferative, proapoptotic, and antiangiogenic effects in tumours that overexpress EGFR (Crombet-Ramos *et al*, 2002). In early clinical trials, nimotuzumab has shown a longer half-life and a greater area under the curve (AUC) in comparison with other anti-EGFR antibodies (Crombet *et al*, 2003). A phase I/II trial showed that nimotuzumab was well tolerated and enhanced the curative potential of radiation in patients with advanced head and neck cancer (Crombet *et al*, 2004). Given that little is known of the antitumor action of nimotuzumab in NSCLC, we investigated the growth-inhibitory effects of this mAb alone and in combination with radiation in NSCLC cell lines with differing patterns of EGFR expression. We also examined whether genetic alterations of *EGFR* affect the antitumor action of combined treatment with nimotuzumab and radiation.

MATERIALS AND METHODS

Cell lines and reagents

The human NSCLC cell lines NCI-H292 (H292), NCI-H460 (H460), Ma-1, NCI-H1299 (H1299), and NCI-H1975 (H1975) were obtained as previously described (Okabe *et al*, 2007) and were maintained under a humidified atmosphere of 5% CO_2 in air at 37.0°C in RPMI 1640 medium (Sigma, St Louis, MO, USA) supplemented with 10% fetal bovine serum and 1% penicillin–streptomycin. Nimotuzumab was provided by Daiichi Sankyo Co Ltd (Tokyo, Japan), and gefitinib was obtained from AstraZeneca (Macclesfield, UK).

Flow cytometric analysis of surface EGFR expression

Cells (1.0×10^6) were stained for 2 h at 4°C with an R-phycoerythrin-conjugated mAb to EGFR (BD Biosciences, San Jose, CA, USA) or an isotype-matched control mAb (BD Biosciences). The cells were washed three times before measurement of fluorescence with a flow cytometer (FACScalibur; Becton Dickinson, San Jose, CA, USA).

Immunoblot analysis

Cell lysates were fractionated by SDS-polyacrylamide gel electrophoresis on a 7.5% gel, and the separated proteins were transferred to a nitrocellulose membrane. After blocking of nonspecific sites, the membrane was incubated consecutively with primary and secondary antibodies, and immune complexes were detected with the use of enhanced chemiluminescence reagents, as described previously (Okabe *et al*, 2007). Primary antibodies to phosphorylated EGFR (pY1068) were obtained from Cell Signaling Technology (Beverly, MA, USA), and those to EGFR were from Zymed (South San Francisco, CA, USA). Horseradish peroxidase-conjugated goat secondary antibodies were obtained from Amersham Biosciences (Little Chalfont, UK).

Clonogenic assay

Exponentially growing cells in 25-cm^2 flasks were harvested by exposure to trypsin and counted. They were diluted serially to appropriate densities and plated in triplicate in 25-cm^2 flasks containing 10 ml of medium supplemented with 1% fetal bovine serum in the absence or presence of 700 nM nimotuzumab. After incubation for 24 h, the cells were exposed to various doses of γ-radiation with a ^{60}Co irradiator at a rate of approximately 0.82 Gy min^{-1} and at room temperature. The cells were then washed with phosphate-buffered saline, cultured in drug-free medium for 10–14 days, fixed with methanol : acetic acid (10 : 1, v/v), and stained with crystal violet. Colonies containing > 50 cells were counted. The surviving fraction was calculated as (mean number of colonies)/(number of inoculated cells × plating efficiency). Plating efficiency was defined as the mean number of colonies divided by the number of inoculated cells for control cultures not exposed to nimotuzumab or radiation. The surviving fraction for combined treatment was corrected by that for nimotuzumab treatment alone. The dose enhancement factor was then calculated as the dose (Gy) of radiation that yielded a surviving fraction of 0.5 for vehicle-treated cells divided by that for nimotuzumab-treated cells (after correction for drug toxicity).

Antitumor activity of nimotuzumab with or without radiation *in vivo*

Animal experiments were performed in accordance with the Recommendations for Handling of Laboratory Animals for Biomedical Research, compiled by the Committee on Safety and Ethical Handling Regulations for Laboratory Animal Experiments, Kyoto University, and they met the requirements of the UKCCCR guidelines (Workman *et al*, 1998). Tumour cells (2×10^6) were injected subcutaneously into the right hind leg of 7-week-old female athymic nude mice. tumour volume was determined from caliper measurement of tumour length (L) and width (W) according to the formula $LW^2/2$. Treatment was initiated when tumours in each group achieved an average volume of approximately 170–200 mm^3. Treatment groups consisted of control, nimotuzumab alone, radiation alone, and the combination of nimotuzumab and radiation, with each group containing seven or eight mice. Nimotuzumab was administered intraperitoneally in a single dose of 1.0 mg per mouse; mice in the control and radiation-alone groups were injected with vehicle (physiological saline). Tumours in the right hind leg of mice were exposed to 10 Gy of γ-radiation with a ^{60}Co irradiator at a rate of approximately 0.32 Gy min^{-1} beginning 6 h after drug treatment. Growth delay (GD) was calculated as the time required for treated tumours to achieve a fivefold increase in volume minus the corresponding time required for control tumours. The enhancement factor was then determined as $(GD_{combination} - GD_{nimotuzumab})/(GD_{radiation})$.

RESULTS

Surface EGFR expression in NSCLC cell lines of differing *EGFR* status

We first examined the surface expression of EGFR in five NSCLC cell lines by flow cytometry. The *EGFR* status for the cell lines was determined in our previous study (Okabe *et al*, 2007). Three cell lines (H460, H292, and H1299) possess wild-type *EGFR* alleles, whereas the other two cell lines (Ma-1 and H1975) harbour *EGFR* mutations (Table 1). Ma-1 cells have an in-frame deletion in

Table 1 Characteristics of NSCLC cell lines

Cell line	EGFR surface expression	*EGFR* status
H460	Low	Wild type
H292	High	Wild type
H1299	Low	Wild type
Ma-1	Moderate	del(E746–A750)
H1975	Low	L858R/T790M

EGFR = epidermal growth factor receptor; NSCLC = non-small cell lung cancer

exon 19 (E746–A750). H1975 cells harbour the L858R mutation in exon 21 and a secondary mutation in exon 20 (T790M). Activating mutations in exons 19 and 21 are associated with sensitivity to EGFR-TKIs (Lynch *et al*, 2004; Paez *et al*, 2004; Pao *et al*, 2004; Cappuzzo *et al*, 2005; Mitsudomi *et al*, 2005; Takano *et al*, 2005), whereas the T790M mutation contributes to the development of resistance to these drugs (Kobayashi *et al*, 2005; Pao *et al*, 2005). Our flow cytometric analysis demonstrated that H292 and Ma-1 cells express high and moderate levels of EGFR on the cell surface, respectively, whereas H460, H1299, and H1975 cells showed a low level of surface EGFR expression (Figure 1).

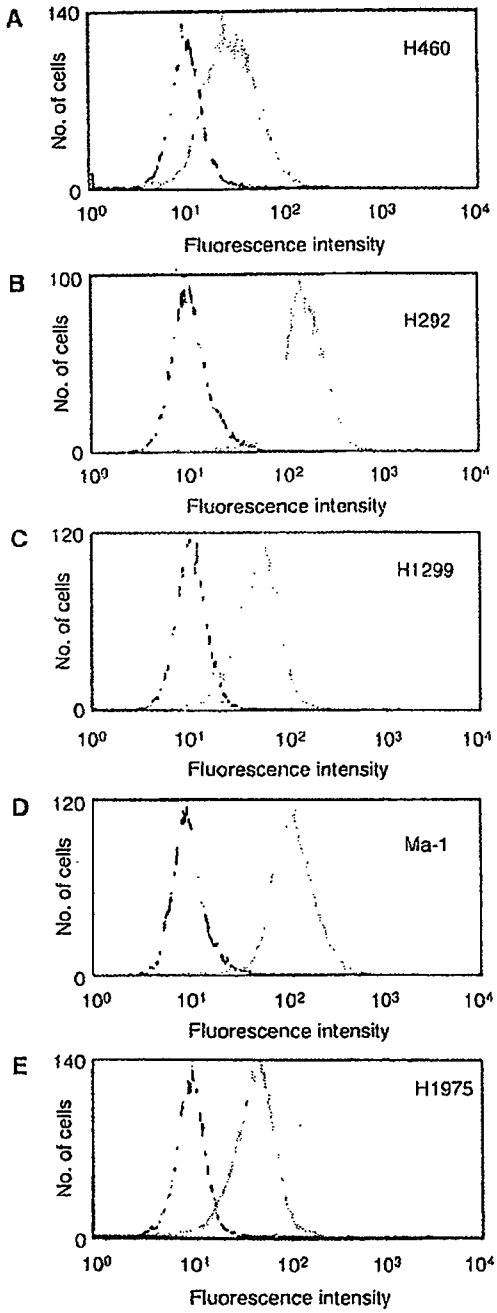

Figure 1 Expression of EGFR on the surface of NSCLC cells. Surface expression of EGFR on H460 (**A**), H292 (**B**), H1299 (**C**), Ma-1 (**D**), and H1975 (**E**) cells was determined by flow cytometry. Representative histograms of cells stained with an anti-EGFR mAb (red peak) or with an isotype-matched control mAb (black peak) are shown.

Effect of nimotuzumab on EGFR phosphorylation

Next, we determined whether nimotuzumab inhibits ligand-induced EGFR phosphorylation in the five NSCLC cell lines. The cells were deprived of serum overnight, exposed to various concentrations of nimotuzumab, or to gefitinib, for 15 min, and then stimulated with EGF for 15 min. In the NSCLC cells that harbour wild-type *EGFR* (H460, H292, and H1299), phosphorylation of EGFR was undetectable in the absence of EGF, but was markedly induced on exposure of the cells to this growth factor. The EGF-induced phosphorylation of EGFR in these cells was completely inhibited by the EGFR-TKI gefitinib. Nimotuzumab also inhibited the EGF-induced EGFR phosphorylation in a concentration-dependent manner in H292 cells (which have a high level of surface EGFR expression), whereas it did not substantially affect such phosphorylation in H460 or H1299 cells (both of which have a low level of surface EGFR expression) (Figure 2A–C). We previously showed that the basal level of EGFR phosphorylation was increased in the *EGFR* mutant NSCLC cell lines Ma-1 and H1975, indicative of constitutive activation of the EGFR tyrosine kinase (Okabe *et al*, 2007). The phosphorylation of EGFR in EGF-treated Ma-1 cells (which have a moderate level of surface EGFR expression) was inhibited by gefitinib as well as by nimotuzumab in a concentration-dependent manner (Figure 2D). In contrast, the constitutive activation of EGFR in H1975 cells (which have a low level of surface EGFR expression) was inhibited partially by gefitinib but was unaffected by nimotuzumab (Figure 2E). These results suggested that the inhibition of EGFR phosphorylation by nimotuzumab may be related to the surface expression level of EGFR rather than to the mutational status of *EGFR*.

Augmentation of the cytotoxic effect of radiation in NSCLC cells by nimotuzumab *in vitro*

We examined whether nimotuzumab might enhance the anticancer effect of γ-radiation in the five NSCLC cell lines with the use of a clonogenic assay. Tumour cells were incubated with or without nimotuzumab for 24 h, exposed to various doses of γ-radiation, and then allowed to form colonies in drug-free medium for 10–14 days. Survival curves revealed that, whereas nimotuzumab had no effect on the radiation sensitivity of H460, H1299, or H1975 cells, it enhanced the cytotoxic effect of radiation in H292 and Ma-1 cells, with a dose enhancement factor of 1.5 and 1.3, respectively (Figure 3). These results showed that nimotuzumab increased the radiosensitivity of the NSCLC cell lines with high or moderate levels of surface EGFR expression, consistent with the inhibitory effects of this antibody on EGFR signalling.

Augmentation of the antitumor effect of radiation in NSCLC cells by nimotuzumab *in vivo*

To determine whether the nimotuzumab-induced potentiation of the response of NSCLC cells to radiation observed *in vitro* might also be apparent *in vivo*, we injected three of the cell lines into nude mice to elicit the formation of solid tumours. The mice were then treated with nimotuzumab, radiation, or both modalities. In the H460 xenograft model, tumour growth was inhibited by radiation alone but not by nimotuzumab alone, and the effect of radiation was not promoted by nimotuzumab (Figure 4A). In contrast, radiation and nimotuzumab each inhibited the growth of tumours formed by H292 (Figure 4B) or Ma-1 (Figure 4C) cells during the first few weeks after treatment. Thereafter, the rate of

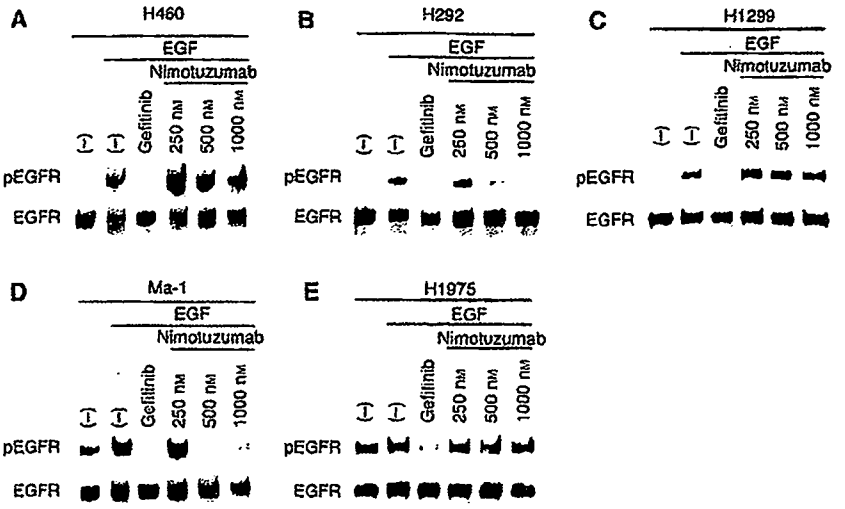

Figure 2 Effect of nimotuzumab on EGFR phosphorylation in NSCLC cells. H460 (**A**), H292 (**B**), H1299 (**C**), Ma-1 (**D**), and H1975 (**E**) cells were deprived of serum overnight and then incubated first for 15 min in the absence or presence of the indicated concentrations of nimotuzumab or gefitinib (10 μM) and then for an additional 15 min in the additional absence or presence of EGF (100 ng ml^{-1}). Cell lysates were then subjected to immunoblot analysis with antibodies to the Tyr1068-phosphorylated form of EGFR (pEGFR) as well as with those to total EGFR.

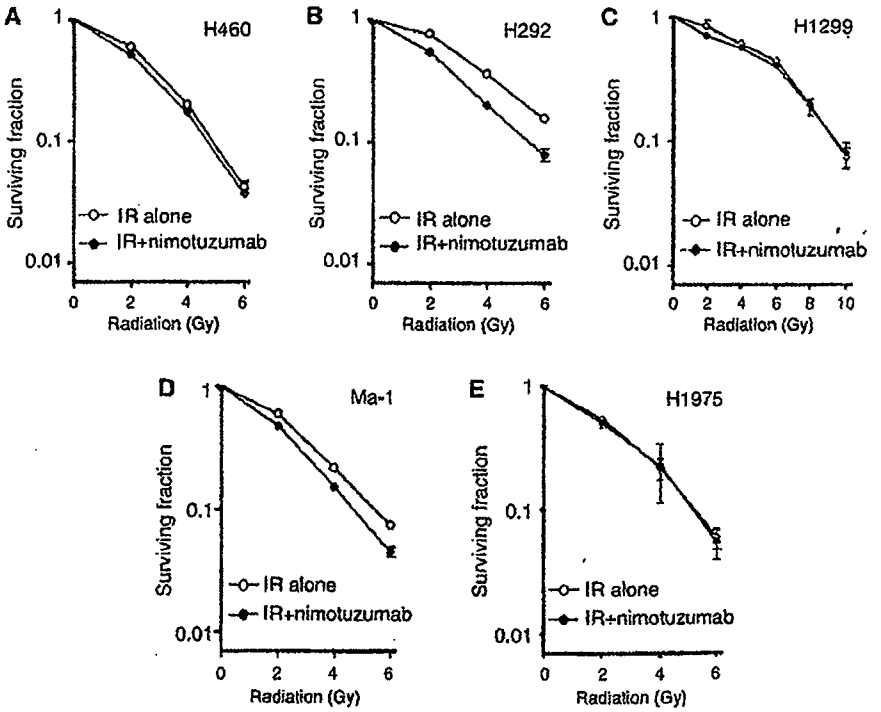

Figure 3 Effect of nimotuzumab on the response of NSCLC cells to radiation *in vitro*. H460 (**A**), H292 (**B**), H1299 (**C**), Ma-1 (**D**), and H1975 (**E**) cells were incubated with or without 700 nM nimotuzumab in medium supplemented with 1% fetal bovine serum for 24 h, exposed to the indicated doses of γ-radiation, and then incubated in drug-free medium supplemented with 10% serum for 10–14 days for determination of colony-forming ability. Survival curves were generated after correction of colony formation observed for combined treatment with ionising radiation (IR) and nimotuzumab by that apparent for treatment with nimotuzumab alone. Data are means ± s.d. of triplicates from a representative experiment.

tumour growth increased to a value similar to that seen in control animals. Combined treatment with radiation and nimotuzumab resulted in a substantial delay in tumour growth and subsequent inhibition of the growth rate of H292 and Ma-1 xenografts. The growth delay after treatment with nimotuzumab alone, radiation alone, or both nimotuzumab and radiation was thus 27.2, 19.6, and 53.6 days, respectively, for H292 cells and 26.7, 13.0, and 78.3 days, respectively, for Ma-1 cells (Table 2). The enhancement factor for the effect of nimotuzumab on the efficacy of radiation was 1.3 for H292 cells and 4.0 for Ma-1 cells, revealing the effect to be more

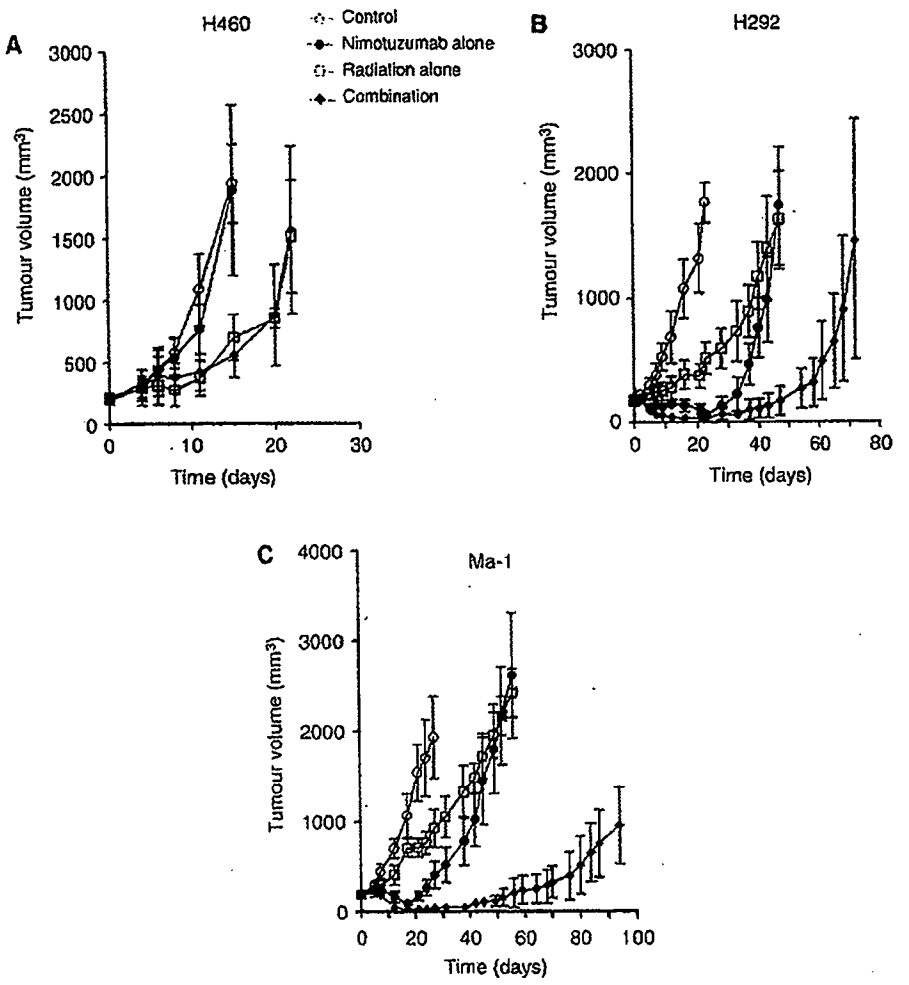

Figure 4 Effect of nimotuzumab on the response of NSCLC cells to radiation *in vivo*. H460 (**A**), H292 (**B**), or Ma-1 (**C**) cells were injected subcutaneously in athymic nude mice. Treatment was initiated when tumours in each group achieved an average volume of approximately 170–200 mm^3. Mice were treated with a single dose of nimotuzumab (1.0 mg per mouse) intraperitoneally, a single dose of γ-radiation (10 Gy), or neither (control) or both modalities, and tumour volume was determined at the indicated time points thereafter. Data are means ± s.d. for seven to eight mice per group.

Table 2 Tumour growth delay in nude mice treated with nimotuzumab, radiation, or both modalities

	H460		H292		Ma-1	
Treatment	**Days[a]**	**GD[b]**	**Days**	**GD**	**Days**	**GD**
Control	10.4		13.2		15.1	
Nimotuzumab alone	11.8	1.4	40.4	27.2	41.8	26.7
Radiation alone	20.4	10.0	32.8	19.6	28.1	13.0
Nimotuzumab+radiation	20.5	10.1	66.8	53.6	93.4	78.3
Enhancement factor	0.86		1.3		4.0	

GD = growth delay [a]Time required for xenografts in each group to achieve a fivefold increase in volume. [b]The additional time (days) required for xenografts in each treatment group to achieve a fivefold increase in volume relative to the corresponding time for xenografts in the control group.

than additive. No pronounced tissue damage or toxicities such as diarrhoea or a decrease in body weight of >10% were observed in mice in any of the four treatment groups. These results thus suggested that nimotuzumab potentiated the antitumor activity of radiation in H292 and Ma-1 cells *in vivo* as well as *in vitro*.

DISCUSSION

Somatic mutations in the EGFR kinase domain and *EGFR* amplification have been associated with a better response to EGFR-TKIs, such as gefitinib and erlotinib, in patients with NSCLC (Lynch *et al*, 2004; Paez *et al*, 2004; Pao *et al*, 2004; Cappuzzo *et al*, 2005; Mitsudomi *et al*, 2005; Takano *et al*, 2005). Given that little is known of the relation between such *EGFR* alterations and the response to treatment with anti-EGFR mAbs, we investigated the antitumor effect of combined treatment with the anti-EGFR mAb nimotuzumab and radiation in NSCLC cell lines of differing *EGFR* status.

The antitumor effect of EGFR-specific mAbs has been thought to result from inhibition of ligand binding to EGFR and consequent inhibition of EGFR activation (Li *et al*, 2005; Marshall, 2006). We, therefore, examined the effect of nimotuzumab on EGF-dependent EGFR signalling. Nimotuzumab inhibited the EGF-induced or constitutive phosphorylation of EGFR in H292 and Ma-1 cells (with high and moderate levels of surface EGFR expression, respectively), consistent with the mode of action of this antibody. However, nimotuzumab did not block EGF-induced or constitutive EGFR phosphorylation in H460, H1299, or H1975 cells (all with a

low level of surface EGFR expression). These observations suggest that the inhibitory effect of nimotuzumab on EGFR signalling depends on the expression level of EGFR on the cell surface. A clonogenic cell survival assay revealed that nimotuzumab enhanced the cytotoxic effect of radiation in H292 and Ma-1 cells, but not that in H460, H1299, or H1975 cells. These findings support the notion that the inhibition of EGFR signalling by nimotuzumab is responsible, at least in part, for the enhancement of the cytotoxic effect of radiation by this antibody. Irradiation of tumour cells has been shown to activate EGFR via ligand-independent and ligand-dependent mechanisms, possibly accounting for radiation-induced acceleration of tumour cell repopulation and the development of radioresistance (Schmidt-Ullrich *et al*, 1997, 2003; Dent *et al*, 2003). Such radiation-induced activation of EGFR-dependent processes may represent a rationale for combined treatment with radiation and EGFR inhibitors. It remains to be determined whether nimotuzumab is able to block radiation-induced activation of EGFR.

Consistent with our *in vitro* results, we found that nimotuzumab enhanced the antitumor effect of radiation on H292 or Ma-1 cells in nude mice. Such enhancement was not apparent for tumours formed by H460 cells. Nimotuzumab alone also manifested a substantial antitumor effect for xenografts formed by H292 or Ma-1 cells but not for those formed by H460 cells. Together these results suggest that the efficacy of nimotuzumab monotherapy is a prerequisite for augmentation of radioresponse by this mAb. Nimotuzumab was previously shown to induce the regression of A431 tumour xenografts *in vivo* as a result of inhibition of both tumour cell proliferation and tumour angiogenesis (Crombet-Ramos *et al*, 2002). Immunohistochemical analysis of tumour specimens from head and neck cancer patients treated with the combination of nimotuzumab and radiation also showed evidence of antiproliferative and antiangiogenic effects (Crombet *et al*, 2004). These observations suggest that effects of nimotuzumab on both NSCLC cell proliferation and tumour angiogenesis might contribute to the enhancement of the antitumor efficacy of radiation by this antibody observed in the present study. Enhancement of the anticancer effect of radiation by the anti-EGFR mAb cetuximab was previously shown to be increased by transfection of cells to upregulate the level of EGFR expression, suggesting that potentiation of the antitumor efficacy of radiation by anti-EGFR mAbs is related to the absolute level of EGFR expression (Liang *et al*, 2003; Bonner *et al*, 2004). This finding is consistent with our present results showing that potentiation of the antitumor activity of radiation by nimotuzumab was related to the level of surface EGFR expression. The nimotuzumab-resistant cell line H460 harbours a mutant form of *KRAS* (Balko *et al*, 2006) that has been associated with resistance to cetuximab (Lievre *et al*, 2006). However, we found that nimotuzumab also failed to inhibit EGF-induced EGFR phosphorylation and to enhance the cytotoxic effect of radiation in H1299 cells, which harbour wild-type *KRAS* (Coldren *et al*, 2006). These observations thus support the notion that a low level of EGFR expression at the cell surface is related to resistance to combined treatment with nimotuzumab and radiation, irrespective of *KRAS* status.

We demonstrated that nimotuzumab inhibited EGFR phosphorylation and enhanced the antitumor effect of radiation in *EGFR* mutant Ma-1 cells (with a moderate level of surface EGFR expression) but not in *EGFR*-mutant H1975 cells (with a low level of surface EGFR expression). Nimotuzumab also potentiated the cytotoxic effect of radiation in H292 cells, which harbour wild-type *EGFR* alleles and have a high level of surface EGFR expression. These findings support the notion that *EGFR* mutation is not the major determining factor for enhancement of the antitumor effect of radiation by nimotuzumab, consistent with previous observations with cetuximab (Barber *et al*, 2004; Tsuchihashi *et al*, 2005). However, the mechanisms underlying such enhancement of the antitumor effect of radiation may differ between NSCLC cells harbouring wild-type or mutant *EGFR* alleles. We and others have previously shown that mutations in the tyrosine kinase domain of EGFR are associated with increased ligand-independent tyrosine kinase activity of EGFR (Lynch *et al*, 2004) and aberrant EGFR signalling (Amann *et al*, 2005; Okabe *et al*, 2007). Given that cell-cycle checkpoints activated by ionising radiation are defective in *EGFR*-mutant NSCLC cell lines (Das *et al*, 2006), the constitutive activity of EGFR in such cells may result in unchecked DNA synthesis and in apoptosis on exposure to ionising radiation. It is possible that these defects in *EGFR*-mutant cells affect the enhancement of the antitumor efficacy of radiation by nimotuzumab.

In summary, we have shown that nimotuzumab enhanced the antitumor efficacy of radiation *in vitro* and *in vivo*, providing a rationale for future clinical investigations of the therapeutic efficacy of nimotuzumab in combination with radiotherapy. Our data suggest that potentiation of the antitumor activity of radiation by nimotuzumab may be related to the level of EGFR expression at the cell surface rather than to *EGFR* mutation. The preselection of patients on the basis of genetic factors that predict treatment sensitivity or resistance may thus be required for the combination therapy with nimotuzumab and radiation.

ACKNOWLEDGEMENTS

We thank S Ono for technical assistance.

REFERENCES

Amann J, Kalyankrishna S, Massion PP, Ohm JE, Girard L, Shigematsu H, Peyton M, Juroske D, Huang Y, Stuart Salmon J, Kim YH, Pollack JR, Yanagisawa K, Gazdar A, Minna JD, Kurie JM, Carbone DP (2005) Aberrant epidermal growth factor receptor signaling and enhanced sensitivity to EGFR inhibitors in lung cancer. *Cancer Res* 65: 226–235

Balko JM, Potti A, Saunders C, Stromberg A, Haura EB, Black EP (2006) Gene expression patterns that predict sensitivity to epidermal growth factor receptor tyrosine kinase inhibitors in lung cancer cell lines and human lung tumors. *BMC Genomics* 7: 289

Barber TD, Vogelstein B, Kinzler KW, Velculescu VE (2004) Somatic mutations of EGFR in colorectal cancers and glioblastomas. *N Engl J Med* 351: 2883

Baselga J (2002) Why the epidermal growth factor receptor? The rationale for cancer therapy. *Oncologist* 7(Suppl 4): 2–8

Baselga J, Arteaga CL (2005) Critical update and emerging trends in epidermal growth factor receptor targeting in cancer. *J Clin Oncol* 23: 2445–2459

Baumann M, Krause M (2004) Targeting the epidermal growth factor receptor in radiotherapy: radiobiological mechanisms, preclinical and clinical results. *Radiother Oncol* 72: 257–266

Bonner JA, Buchsbaum DJ, Russo SM, Piveash JB, Trummell HQ, Curiel DT, Raisch KP (2004) Anti-EGFR-mediated radiosensitization as a result of augmented EGFR expression. *Int J Radiat Oncol Biol Phys* 59: 2–10

Bonner JA, Harari PM, Giralt J, Azarnia N, Shin DM, Cohen RB, Jones CU, Sur R, Raben D, Jassem J, Ove R, Kies MS, Baselga J, Youssoufian H, Amellal N, Rowinsky EK, Ang KK (2006) Radiotherapy plus cetuximab for squamous-cell carcinoma of the head and neck. *N Engl J Med* 354: 567–578

Buchsbaum DJ, Bonner JA, Grizzle WE, Stackhouse MA, Carpenter M, Hicklin DJ, Bohlen P, Raisch KP (2002) Treatment of pancreatic cancer xenografts with Erbitux (IMC-C225) anti-EGFR antibody, gemcitabine, and radiation. *Int J Radiat Oncol Biol Phys* 54: 1180–1193